Finite-Time Estimation and Control for Multi-Aircraft Systems under Wind and Dynamic Obstacles

Kunal Garg* and Dimitra Panagou†
University of Michigan, Ann Arbor, MI 48109

In this paper, we consider the problem of generating safe trajectories for multi-agent systems in the presence of wind and dynamic obstacles. We design a robust controller to counteract a class of state disturbances that can be thought of as wind disturbance for aerial vehicles. The considered disturbance is unmatched, bounded with known bounds, with no assumptions on the regularity properties or the distribution of the disturbance. We also assume that only partial states are observed, and use a finite-time state-estimator based finite-time state-feedback control to generate the system trajectories. We show that even with limited and erroneous sensing, agents are capable of avoiding collisions with moving obstacles and with each other. The designed protocol is distributed, scalable with the number of agents, and provides provable safety and convergence guarantees.

Nomenclature

$\boldsymbol{r}_i$	Position of agent i
$\boldsymbol{u}_i$	Velocity of agent i
$\boldsymbol{a}_i$	Acceleration of agent i
$\boldsymbol{r}_{gi}$	Desired goal location of agent i
$\boldsymbol{w}$	Wind disturbance
$\boldsymbol{w}_{av}$	Mean value of the wind disturbance
δ_{av}	Variation of the wind disturbance from the mean value
d_{ij}	Distance between agent i and j
d_m	Minimum safety distance
R_c	Sensing radius of each agent
δ_e	Estimation error
$\boldsymbol{r}_{js}^i$	Position of agent j as sensed by agent i
$\boldsymbol{u}_{js}^i$	Velocity of agent j as sensed by agent i

*PhD Candidate, Department of Aerospace Engineering, 1320 Beal Avenue, University of Michigan, Ann Arbor, MI 48109. Student Member AIAA.
†Assistant Professor, Department of Aerospace Engineering, 1320 Beal Avenue, University of Michigan, Ann Arbor, MI 48109. Member AIAA.

ϵ_s Sensing error

$\mathbf{F}_i$ Nominal vector field for agent i

γ_i Desired direction of motion for agent i

u_{id} Desired speed for agent i

$\hat{\boldsymbol{r}}_i$ Estimated position of agent i

$\hat{\boldsymbol{u}}_i$ Estimated velocity of agent i

$\hat{\boldsymbol{u}}_{id}$ Desired estimated velocity for agent i

$\hat{d}_{ij}$ Estimated distance between agent i and j

$\mathbb{R}_+$ Set of non-negative reals

$\|\cdot\|$ Euclidean norm (2-norm) of $(\cdot)$

$\angle(\boldsymbol{x})$ Orientation of vector $\boldsymbol{x}$

$\mathbf{0}$ Zero vector

$\emptyset$ Empty set

I. Introduction

A. Motivation

In recent years, the usability of Unmanned Aerial Vehicles (UAVs) has increased due to availability and technology maturity, especially multirotor-type UAVs, which are now used for commercial and consumer applications including package transportation [1] and distributed sensing [2]. Large-scale problems make centralized algorithms intractable with the number of agents, motivating the research in the field of distributed coordination and control. The problem of decentralized multi-agent motion planning, which mainly focuses on generating collision-free trajectories for multiple agents (e.g., UAVs) so that they reach preassigned goal locations under limited sensing, communication, and interaction capabilities has been studied by many researchers [3–5].

In this paper, we consider the problem of safe trajectory generation for multi-rotor type UAVs for low-altitude urban environment operations. Specifically, we seek to generate safe trajectories from every initial condition to any goal location for double integrator vehicles with limited, erroneous sensing capabilities, in the presence of unknown wind disturbance and moving obstacles. Furthermore, we make use of finite-time stability theory so that the agents accomplish the assigned tasks in finite time.

B. Relevant work

Numerous methodologies on distributed motion planning of multi-agent systems have appeared in recent years, with the most popular being (i) optimization-based techniques [6–8]; (ii) Lyapunov-based methods [9, 10]; (iii) Voronoi-based

methods [11, 12]; and (iv) graph search methods, e.g., A^* planning [13], Pareto optimization [14] and sampling-based methods (e.g., RRTs) [15–17]; see also [18, Chapter 2, 6] and [19, Chapter 4, 7]. Lyapunov-based controllers are of particular interest for multi-agent problems, as they are scalable with the number of agents and bring in the merits of Lyapunov-based analysis for safety and convergence guarantees.

Various methods using Lyapunov-like scalar functions have been employed for multi-agent motion planning problems, such as avoidance functions [20], potential functions [21], navigation functions [22, 23] and harmonic functions [24]. The idea of *directly* defining vector fields as feedback motion plans is also well-studied. Relevant work employing vector fields for vehicle navigation can be found in [25–27] and references therein. In [28, 29], the authors consider the problem of collision avoidance for cooperative and non-cooperative agents. However, they only consider the case of two vehicles, with complete knowledge of the state of the vehicle without any external disturbance.

The main issue with sampling-based or graph-based methods is scalability with number of agents. The scalability issues can be circumvented by using Lyapunov-based methods, such as navigation fields. One of the issues with using navigation fields and similar methods (e.g., potential functions) is the possible occurrence of deadlock points or surfaces, wherein the resultant vector field vanishes. In our earlier work [30], we guaranteed *almost global* convergence due to the occurrence of deadlock for a set of initial conditions of measure zero. In this work, we address the problem of avoiding the deadlock entirely by properly defining the direction of motion for the agents when the vector field vanishes, so that we have *global* convergence.

C. Limited and Erroneous Sensing

In the aforementioned work [20–30], it is assumed that each agent has perfect knowledge of its own states as well as of its neighbors' states. From practical and robustness point of view, sensing uncertainties along with the case when only partial state measurements are available should be considered. Another important aspect is the limited capabilities of the considered vehicles, in terms of limited sensing and communication radii. From the safety perspective, the agents must be able to avoid collisions with each other and with obstacles under these limitations. In [28], the authors consider limited sensing radius for a pair of nonholonomic vehicles for cooperative and non-cooperative collision avoidance. In [23], the authors used potential functions for formation control and obstacle avoidance under limited sensing. In [31] (see also [32]), the authors design a centralized *supervisor* for collision avoidance in the presence of disturbances and uncontrolled vehicles. However, the work in [23, 28, 31, 32] assumes complete knowledge of the states of the agents and no sensing uncertainties. In this work, we design a robust controller that guarantees safety and convergence when only partial state measurements are available, and there are sensing uncertainties in both the position and velocity of each agent.

D. Disturbance Modeling

Ensuring certain levels of robustness against modeling uncertainties and external disturbances is of primary concern for real-world applications. Much work is done for the case of matched disturbances, i.e., when the control input and the disturbance enter the plant via the same channel. In [33], a stable uncertainty is assumed to be bounded in $\mathcal{H}_\infty$-norm by some *prior* given desired tolerance, and an observer-based controller is designed by using the algebraic Riccati equation. Related work considering bounded deterministic disturbances can be found in the design of finite-time consensus algorithms with matched disturbances [34–36], mismatched disturbances [37], and the rotating consensus control with mixed model uncertainties and external disturbances [38].

Wind, modeled as a state-disturbance, affects the position trajectories of the aerial vehicles. For most of the practical systems, such as fixed-wing (or rotary wing) aircraft, the control inputs are the deflection of control surfaces and thrust (or the rotor-speed), which take effect in the velocity dynamics of the vehicle. Hence, the study of systems with unmatched disturbance becomes significantly important. Nevertheless, there is only little work in this field: in [39], the authors assumed that the dynamics of the unmatched disturbance are known, and leverage this knowledge to design a disturbance observer. In [40], the authors assumed that the disturbance is an element of $\mathcal{L}_\infty$. In [41] and [42], the authors assumed that the disturbance satisfies a strong regularity condition that the disturbance should be at least twice differentiable for a second order system, and that all the derivatives of the disturbance are bounded with known bounds. While under these *strong* assumptions, the aforementioned work showed that the effect of the disturbance can be nullified, it is worth noting that one cannot always assume such smoothness or vanishing properties for wind disturbances. In our earlier work [43, 44], the wind disturbance was modeled as Gaussian disturbance with known mean and variance. We relax this assumption by allowing the wind to have any arbitrary distribution, which we do not assume to be known. Instead, we assume a general class of state disturbances, that can vary both in space and time and, unlike [39–44], we assume that only the mean value and the maximum deviation of the disturbance from the mean value are known.

E. Finite-time Stability in Multi-Agent Systems

It is often desired that agents achieve their task of reaching given locations in finite time. Also, for estimator-based full-state feedback, the convergence of estimation error in finite time is desired. *Finite-Time Stability* (FTS) is a well-studied concept, motivated in part from a practical viewpoint due to properties such as achieving convergence in finite time, as well as exhibiting robustness with respect to disturbances [45]. The authors in [46] focus on continuous autonomous systems and present Lyapunov-like necessary and sufficient conditions for a system to exhibit FTS, whereas [47] they provide geometric conditions for homogeneous systems to exhibit FTS. Finite-time controllers have been used for applications such as consensus or formation control in [48–50], but without any consideration of safety or collision avoidance.There is a large body of literature on collision avoidance schemes along with finite-time convergence, e.g., [51–53] consider finite-time consensus with inter-agent collision avoidance, whereas [54] incorporates collision

avoidance in finite-time flocking of *Cucker-smale* agents. [55] considers problem of parallel formation (or, velocity alignment) in finite time in a stationary-obstacle environment. Although the aforementioned work considers inter-agent collision avoidance or obstacle avoidance, none of them consider any external disturbances or uncertainties in the state measurements. [56] considers bounded, matched disturbance and presents a method of achieving robust finite-time consensus for multi-agent systems. Recent work such as [35, 36] consider bounded, matched disturbances, whereas [57] considers unknown non-linearities in the dynamics, and design protocols to achieve consensus in a *fixed time*. However, [35, 36, 56, 57] do not consider collision avoidance. In this paper, we consider finite-time convergence in the presence of external disturbances and sensor uncertainties, along with collision avoidance of the agents with each other and with dynamic obstacles.

F. Contributions of paper

We consider the motion of *class-A* or controlled agents in a dynamic obstacle environment induced by *class-B* or uncontrolled agents (or simply, dynamic obstacles), as defined in [30]. The dynamic obstacles do not cooperate to avoid collisions. Compared to our earlier work [30], where the agents were modeled as unicycles to capture the no-slip condition for car-like vehicles, here we model the agents using double integrator dynamics for 2-D motion of multi-rotor aircraft. In [30], perfect communication between the agents was assumed and each agent had knowledge of whether the neighboring agents are cooperative or non-cooperative. In this paper, 1) the agents do not know whether their neighbors are cooperative or non-cooperative and 2) there is no active communication between the agents. We rather assume a limited sensing model that is erroneous, i.e., the agents can sense position and velocity of their neighboring agents with some bounded error. Also, in contrast to [58] where the *nominal*, disturbance-free case was treated, we consider a general class of unmatched, state disturbances in the agents' dynamics to account for wind disturbances. Furthermore, in contrast to our prior work [30, 58] where all the states were assumed to be known, here we assume that only position measurements are available and make use of a state-estimator for the control design of the agents. We design an FTS state-feedback control law that uses state estimates derived from an FTS state-estimator. *To the best of our knowledge, this is the first time an estimator-based finite-time feedback controller is used in the presence of disturbances and moving obstacles with safety considerations for multi-agent systems*. Also, in contrast to any of the prior work of the authors where only *almost* global convergence was guaranteed, here we design a novel way of defining the desired direction of motion that eliminates the deadlock situation and guarantees global convergence.

In summary, the contributions of this paper are as follows: (i) we present a robust, distributed coordination protocol that accommodates a class of unknown, bounded, unmatched disturbances in the agents' dynamics (the disturbance can have spatial as well as temporal variation) (ii) we treat the case of dynamic obstacles with bounded speeds and prove safety of the system under sensing errors and external disturbances; (iii) we consider limited, erroneous sensing and provide safety guarantees; (iv) we make use of an estimator-based feedback for the case when only partial state

measurements are available; (v) we make use of finite-time stability theory for both state-estimation and state-feedback control design for better performance, both in terms of convergence and disturbance rejection; (vi) we use a novel desired direction of motion for the agents' planning and control so that provable safety and global convergence guarantees can be obtained; and (vii) our proposed vector field method is distributed and is scalable with the number of agents.

G. Organization of the Paper

In Section II, we provide an overview of the modeling of the system under the effect of disturbances. We first present the vector field design for each agent i, which is by construction safe and convergent, and then design a state-feedback controller so that agents follow their respective vector fields in the *nominal* case, i.e., when there is no external disturbance and complete state information is available. In Section III, we present the robust observer-based control design. We first design a finite-time observer to reconstruct the state when only partial states are observed. Then we design the robust controller using the estimated states, and prove safety and convergence of the system. In Section IV, we treat the case of dynamic obstacles. using the controller from Section III, we design a safe protocol that assures collision avoidance with dynamic obstacles. In Section V, we present the simulation results and in Section VI, we discuss the performance of the designed protocol. Conclusions are summarized in Section VII.

II. Modeling and Problem Statement

Consider N identical agents $i \in \{1, \dots, N\}$, that are assigned to move to goal locations of position coordinates $\boldsymbol{r}_{gi} = \begin{bmatrix} x_{gi} & y_{gi} \end{bmatrix}^T$ while avoiding collisions, i.e., for all agents $i \neq j$, $\|\boldsymbol{r}_i(t) - \boldsymbol{r}_j(t)\| \geq d_m$ for all $t \geq 0$, where d_m is a user-defined safety distance. Each agent i is assumed to be a multi-rotor aircraft whose equations of motion for 2-D planar motion are approximated via double integrator dynamics. In this paper, we restrict the motion of the agents to 2-D (or planar) motion. One of the main reasons for this constraint is that we are considering the problem of safe trajectory generation of multi-rotor aircraft flying in a low-altitude urban airfield with restrictions on the airspace available for such operations, particularly in terms of altitude restrictions. With the anticipated increase in the number of vehicles in the airspace, it might be desired to have altitude bands designated to different classes of UAVs depending upon their capabilities. Thus, it is of interest to design safe trajectories of the aircraft with fixed altitude constraints. Hence, we use the following dynamics to model the motion of the agents:

$$\dot{\boldsymbol{r}}_i(t) = \boldsymbol{u}_i(t) + \boldsymbol{w}(\boldsymbol{r}_i(t), t), \tag{1a}$$

$$\dot{\boldsymbol{u}}_i(t) = \boldsymbol{a}_i(t), \tag{1b}$$

$$\boldsymbol{y}_i(t) = \boldsymbol{r}_i(t), \tag{1c}$$

where $\boldsymbol{r}_i(t) = \begin{bmatrix} x_i(t) & y_i(t) \end{bmatrix}^T$ is the position vector of agent i, $\boldsymbol{y}_i(t)$ is the output map of the system consisting of the position of agent i, $\boldsymbol{u}_i(t) = \begin{bmatrix} u_{ix}(t) & u_{iy}(t) \end{bmatrix}^T$ is the velocity vector comprising the linear velocities of the agent i and $\boldsymbol{a}_i(t) = \begin{bmatrix} a_{ix}(t) & a_{iy}(t) \end{bmatrix}^T$ is the acceleration input to agent i. The term $\boldsymbol{w}(\boldsymbol{r}_i, t) : \mathbb{R}^2 \times \mathbb{R}_+ \to \mathbb{R}^2$ is the unknown wind disturbance, which can vary in space and time. As can be seen from (1), the disturbance $\boldsymbol{w}(\boldsymbol{r}_i, t)$ is unmatched. We make the following assumption about the disturbance $\boldsymbol{w}(\boldsymbol{r}, t)$.

Assumption 1. *The norm of the wind disturbance is bounded as*

$$\|\boldsymbol{w}(\boldsymbol{r}, t) - \boldsymbol{w}_{av}\| \leq \delta_w \quad \forall (\boldsymbol{r}, t) \in \mathcal{D} \subseteq \mathbb{R}^2 \times \mathbb{R}_+ \tag{2}$$

where $\boldsymbol{w}_{av} = \frac{\int_{\mathcal{D}} \boldsymbol{w}(\boldsymbol{r},t) d\boldsymbol{s}}{\int_{\mathcal{D}} d\boldsymbol{s}}$ *is the average or mean value of the disturbance with* $\|\boldsymbol{w}_{av}\| < \infty$ *and* $\delta_w < \infty$ *is the maximum deviation of the disturbance from the mean value. Furthermore, the parameters* $\boldsymbol{w}_{av}$ *and* δ_w *are known.*

Remark 1. We only assume that the disturbance is bounded with known bound and known mean value. Our assumptions on the unmatched disturbance $\boldsymbol{w}(\boldsymbol{r}, t)$ are much less conservative as compared to the following literature: (i) in [39], the authors assume that the dynamics of the disturbance are known; (ii) in [40], the authors assume that the disturbance is an element of $\mathcal{L}_\infty$; (iii) in [41], the authors assumed that the disturbance satisfies a stronger regularity assumption, i.e., it should be at least twice differentiable for double-integrator systems.

Each agent i has a circular sensing region C_i of radius R_c centered at $\boldsymbol{r}_i = \begin{bmatrix} x_i & y_i \end{bmatrix}^T$, denoted as $C_i : \{\boldsymbol{r} \in \mathbb{R}^2 \mid \|\boldsymbol{r}_i - \boldsymbol{r}\| \leq R_c\}$. We denote by $\mathcal{N}_i = \{j \mid \boldsymbol{r}_j \in C_i\}$ the set of agents that are in the sensing region of agent i, and call them neighbors of agent i. Agent i can sense the position and velocity of any neighbor $j \in \mathcal{N}_i$. To this end, we make the following assumption on the sensing error for each agent i.

Assumption 2. *Agent i can sense the position (denoted as $\boldsymbol{r}^i_{js}$) and velocity (denoted as $\boldsymbol{u}^i_{js}$) of any agent $j \in \mathcal{N}_i$ within a bounded error ϵ_s, i.e., $\|\boldsymbol{r}_j(t) - \boldsymbol{r}^i_{js}(t)\| \leq \epsilon_s$ and $\|\boldsymbol{u}_j(t) - \boldsymbol{u}^i_{js}(t)\| \leq \epsilon_s$.*

Also, we make the following assumption on the initial and goal location of the agents and the sensing radius R_c to ensure safety and convergence.

Assumption 3. *For each pair (i, j) such that $i \neq j$, $\|\boldsymbol{r}_i(0) - \boldsymbol{r}_j(0)\| > d_s$ and $\|\boldsymbol{r}_{gi} - \boldsymbol{r}_{gj}\| \geq 2R_c$, where d_s is the modified safety distance as defined in Theorem 5. Furthermore, the sensing radius satisfies $R_c > 2d_s$.*

For each agent i, we design a vector-field-based feedback controller. First, we design a vector field that can steer the agents towards their goal locations while maintaining safe inter-agent distances. Then, we design a feedback law to follow this vector field, as per our prior work in [30]. For the sake of brevity, the explicit dependence on time is dropped in the following sections.

A. Vector Field Design

We seek two categories of vector fields to achieve our objectives.

Attractive vector field: We use a radially attractive vector field that navigates agent i towards its goal location $\boldsymbol{r}_{gi}$, given as:

$$\mathbf{F}_{gi} = -\frac{(\boldsymbol{r}_i - \boldsymbol{r}_{gi})}{\|\boldsymbol{r}_i - \boldsymbol{r}_{gi}\|}. \tag{3}$$

Vector field (3) is globally attractive, which ensures that whenever agent i is conflict-free, i.e., $\mathcal{N}_i = \emptyset$, it moves towards its goal location. Note that at $\boldsymbol{r}_i = \boldsymbol{r}_{gi}$, the vector field $\mathbf{F}_{gi}$ is defined to be $\mathbf{0}$, so that it is defined everywhere on $\mathbb{R}^2$.

Repulsive vector field: In order to maintain a safe distance from agent $j \in \mathcal{N}_i$, agent i operates under a radially-repulsive field $\mathbf{F}_{ij}$ given by:

$$\mathbf{F}_{ij} = \frac{\boldsymbol{r}_i - \boldsymbol{r}_j}{\|\boldsymbol{r}_i - \boldsymbol{r}_j\|}. \tag{4}$$

This is a radially repulsive field, which makes agent i move away from any agent $j \in \mathcal{N}_i$.

B. Blending attractive and repulsive vector fields

Let $d_{ij} = \|\boldsymbol{r}_i - \boldsymbol{r}_j\|$ be the inter-agent distance between agent i and j. Since we assume limited sensing radius R_c for agent i and we require agent i to maintain d_m as the minimum separation from all the other agents, we design the following *bump-function* $\sigma_{ij}(\cdot) : \mathbb{R}_+ \to [0, 1]$ to blend the attractive and repulsive fields [30]:

$$\sigma_{ij}(d_{ij}) = \begin{cases} 1, & d_m \leq d_{ij} < d_r; \\ a\ {d_{ij}}^3 + b\ {d_{ij}}^2 + c\ d_{ij} + d, & d_r \leq d_{ij} \leq R_c; \\ 0, & d_{ij} > R_c; \end{cases} \tag{5}$$

where d_r is a positive constant such that $d_m < d_r < R_c$. The coefficients a, b, c, d have been computed as: $a = -\frac{2}{(d_r - R_c)^3}$, $b = \frac{3(d_r + R_c)}{(d_r - R_c)^3}$, $c = -\frac{6\ d_r R_c}{(d_r - R_c)^3}$ and $d = \frac{{R_c}^2(3d_r - R_c)}{(d_r - R_c)^3}$, so that the bump function σ_{ij} given as per (5) is a C^1 function.

One may now define the vector field for each agent i as:

$$\mathbf{F}_i = \sum_{j \in \mathcal{N}_i} \sigma_{ij} \mathbf{F}_{ij} + \prod_j (1 - \sigma_{ij}) \mathbf{F}_{gi}. \tag{6}$$

The blending of the vector fields according to (6) means that whenever agent i is far away from all the other agents, i.e., $d_{ij} > R_c$ for all j, then only the globally attractive vector field is active, whereas if there are other agents in its vicinity, the net vector field is a weighted average of the attractive field $\mathbf{F}_{gi}$ and the repulsive field $\mathbf{F}_{ij}$, and, in the case when

there is an agent j very close to the agent i, i.e., $d_{ij} < d_r$, then only the repulsive vector field $\mathbf{F}_{ij}$ is active.

The controller objective is to design a controller $\boldsymbol{a}_i$ for each agent i, so that the motion of each agent i is along the vector field $\mathbf{F}_i$. We design the desired velocity $\boldsymbol{u}_{id}$ to be tracked with its direction $\angle \boldsymbol{u}_{id}$ along (6) and we design its magnitude $\|\boldsymbol{u}_{id}\|$ so that the safety is ensured at all times. The desired direction of motion of agent i is set to be:

$$\gamma_i = \begin{cases} \tan^{-1}\left(\frac{\mathbf{F}_{iy}}{\mathbf{F}_{ix}}\right), & \|\mathbf{F}_i\| > 0; \\ \tan^{-1}\left(\frac{x_i - x_{gi}}{-(y_i - y_{gi})}\right), & \|\mathbf{F}_i\| = 0. \end{cases} \tag{7}$$

Note that $\tan^{-1}\left(\frac{x_i - x_{gi}}{-(y_i - y_{gi})}\right)$ is the orientation of the vector perpendicular to the vector $\boldsymbol{r}_i - \boldsymbol{r}_{gi}$ pointing to its right. We define this desired direction for the case when $\|\mathbf{F}_i\| = 0$ so that there is no deadlock, as showed in the following lemma. Let $\gamma_i^0 \triangleq \tan^{-1}\left(\frac{x_i - x_{gi}}{-(y_i - y_{gi})}\right)$.

Lemma 1. *There is no deadlock, i.e., the agents would not get stuck, at any location other than their goal location $\boldsymbol{r}_{gi}$ for all times, if the direction of the motion of each agent i is along γ_i given by* (7)*.*

Proof. See Appendix A. □

We next design a desired velocity command with magnitude u_{id} and direction $\boldsymbol{u}_{idn} = \begin{bmatrix} \cos\gamma_i & \sin\gamma_i \end{bmatrix}^T$ for each agent i, which tracks the vector field (6), so that the trajectories of the agent i are collision-free and reach the goal location $\boldsymbol{r}_{gi}$. We then consider the error between the actual velocity $\boldsymbol{u}_i$ and the desired linear velocity $\boldsymbol{u}_{id}$ of agent i, and design an acceleration controller $\boldsymbol{a}_i$ that drives this error to zero in finite-time. We ensure that the safety is maintained by enlarging the safety distance d_m by the maximum transient error induced by the velocity error $\boldsymbol{u}_i - \boldsymbol{u}_{id}$.

C. State Feedback Design

In order to design the desired velocity command $\boldsymbol{u}_{id}$ that generates collision-free position trajectories for the kinematic subsystem (1a) of each agent i, we build upon the control design in [9]. In our prior work [58], the desired velocity vector is defined as $\boldsymbol{u}_{id} = u_{id}\boldsymbol{u}_{idn}$ where $\boldsymbol{u}_{idn} = \begin{bmatrix} \cos\gamma_i & \sin\gamma_i \end{bmatrix}^T$ and u_{id} of agent i is set as:

$$u_{id} = \begin{cases} \frac{1}{\mu}\log\left(\left(\sum\limits_{j\in\mathcal{N}_i|J_i<0} e^{-\mu\, u_{i|j}}\right)^{-1} + 1\right), & d_m \le d_{ij} \le R_c; \\ u_{ic}, & d_{ij} > R_c; \end{cases} \tag{8}$$

where $u_{i|j}$ denotes the velocity adjustment mechanism of agent i with respect to (w.r.t.) agent j, defined as:

$$u_{i|j} = u_{ic}\frac{d_{ij} - d_m}{R_c - d_m} + \varepsilon_i u_{is|j}\frac{R_c - d_{ij}}{R_c - d_m}, \tag{9}$$

with the terms in (9) defined as:

$$u_{ic}(\boldsymbol{r}_i) = \begin{cases} k_{i1} \tanh\left(\left\|\boldsymbol{r}_i - \boldsymbol{r}_{gi}\right\|\right), & \|\boldsymbol{r}_i - \boldsymbol{r}_{gi}\| > R_1; \\ k_{i2}\|\boldsymbol{r}_i - \boldsymbol{r}_{gi}\|^{\alpha_r}, & \|\boldsymbol{r}_i - \boldsymbol{r}_{gi}\| \leq R_1; \end{cases}, \tag{10a}$$

$$u_{is|j} = u_{jd} \frac{\boldsymbol{r}_{ji}{}^T \boldsymbol{u}_{jdn}}{\boldsymbol{r}_{ji}{}^T \boldsymbol{u}_{idn}}, \quad J_i = \boldsymbol{r}_{ji}{}^T \boldsymbol{u}_{idn} \tag{10b}$$

where $0 < \alpha_r, \varepsilon_i < 1$, $\boldsymbol{r}_{ji} \triangleq \boldsymbol{r}_i - \boldsymbol{r}_j$, and $\mu \gg 1$ is a large positive number. Note that the term u_{ic} given in (10a) is defined differently from [30, 58], so that we can guarantee finite-time convergence unlike the prior work where only asymptotic convergence was guaranteed. Gains k_{i1}, k_{i2} and parameter R_1 are chosen such that u_{ic} is continuously differentiable for all $\boldsymbol{r}_i$. Hence, enforcing continuity of u_{ic} and its derivative when $\|\boldsymbol{r}_i - \boldsymbol{r}_{gi}\| = R_1$, we have:

$$k_{i1} \tanh R_1 = k_{i2} R_1^{\alpha_r} \quad \text{and} \quad k_{i1}(1 - \tanh^2 R_1) = \alpha_r k_{i2} R_1^{\alpha_r - 1}. \tag{11}$$

From the above equations, we obtain R_1 as the solution of

$$(1 - \tanh^2 R_1) = \alpha_r \frac{\tanh(R_1)}{R_1}. \tag{12}$$

The above expression has a unique positive solution R_1 for any $0 < \alpha_r < 1$. For a given positive gain $k_{i1} > 0$, k_{i2} is given as $k_{i2} = k_{i1} \frac{\tanh R_1}{R_1^{\alpha_r}}$. The term $\|\boldsymbol{r}_i - \boldsymbol{r}_{gi}\|^{\alpha_r}$ ensures finite-time convergence (Theorem 6). We use (10a) so that the magnitude of the desired speed u_{ic} is bounded for all $\boldsymbol{r}_i$.

Remark 2. The expression given in (8) is a smooth approximation of the following function

$$\max\left\{0, \min_{k \in \mathcal{N}_i | J_k < 0} u_{i|k}\right\}.$$

We first approximate the min function by $g(a) = -\frac{1}{\mu}\log(\sum_i e^{-\mu a_i})$ with $\mu \gg 1$ where $a = \begin{bmatrix} a_1 & a_2 & \cdots a_l \end{bmatrix}$. Using the smooth approximation for max function $h(b) = \frac{1}{\mu}\log(\sum_i e^{\mu b_i})$ for $b = \begin{bmatrix} g(a) & 0 \end{bmatrix}$, we have that $h(b) = \frac{1}{\mu}\log(e^{\mu g(a)} + 1)$. Using the fact that $e^{\mu g(a)} = e^{-\log(\sum_i e^{-\mu a_i})} = (\sum_i e^{-\mu a_i})^{-1}$, we obtain the expression as in (8).

Remark 3. Note that the desired velocity in (8) assumes that agent i has perfect knowledge of its neighbour j's position and velocity. We relax this assumption in the robust control design (Section III). Also, we do not use the protocol defined in (8) directly, but we built upon it for the case of robust controller design. We include equation (8) here, taken directly from [30], for the sake of completeness.

With this desired velocity in hand, the acceleration command is chosen to be

$$\boldsymbol{a}_i = \dot{\boldsymbol{u}}_{id} - \lambda_i(\boldsymbol{u}_i - \boldsymbol{u}_{id})\|\boldsymbol{u}_i - \boldsymbol{u}_{id}\|^{\alpha-1}, \tag{13}$$

where $\lambda_i > 0$, $0 < \alpha < 1$ so that the velocity error $\boldsymbol{u}_i - \boldsymbol{u}_{id}$ converges to $\mathbf{0}$ in finite time *. Since in this paper, we assume that only the position of agent i is measured, we first design a state-estimator in order to be able to implement full-state feedback. Then, we re-design the desired velocity command (denoted as $\hat{\boldsymbol{u}}_{id}$) for the estimator dynamics so that it is robust w.r.t. to the state-disturbance $\boldsymbol{w}(\boldsymbol{r}, t)$ and sensing uncertainties.

III. Robust Control Design

A. Overview of finite-time stability

We first define the notion of finite-time stability and present some related results.

Definition 1. *[46] The origin of the system $\dot{\boldsymbol{x}}(t) = \boldsymbol{f}(\boldsymbol{x}(t))$ is called an FTS equilibrium (or, simply, FTS) if, in some domain $\mathcal{D} \subseteq \mathbb{R}^n$ containing the origin, it is stable in the sense of Lyapunov; and it is finite-time converging, i.e., there exists a finite-time T such that $\lim_{t\to T} \boldsymbol{x}(t) = \mathbf{0}$. Furthermore, if these conditions hold globally, i.e., $\mathcal{D} = \mathbb{R}^n$, then the origin is called globally FTS equilibrium (or, simply, GFTS).*

Theorem 1. *[46] The origin of the system $\dot{\boldsymbol{x}}(t) = \boldsymbol{f}(\boldsymbol{x}(t))$ is FTS if there exists a positive definite function $V(\boldsymbol{x}) : \mathcal{D} \to \mathbb{R}$ such that $\dot{V}(\boldsymbol{x}) + cV(\boldsymbol{x})^\alpha \leq 0$ along the system trajectories for some $c > 0$, $0 < \alpha < 1$ for all $\boldsymbol{x} \in \mathcal{V} \setminus \{\mathbf{0}\}$, where $\mathcal{V} \subseteq \mathcal{D}$ is an open neighbourhood of the origin. If $\mathcal{D} = \mathbb{R}^n$, V is proper and $\dot{V}$ takes negative values for all $\boldsymbol{x} \in \mathbb{R}^n \setminus \{\mathbf{0}\}$, then the origin is GFTS.*

Definition 2. *[47] A function $\boldsymbol{f} : \mathbb{R}^n \to \mathbb{R}^n$ is called a homogeneous function with degree d w.r.t. a dilation function $\Delta_\epsilon(\boldsymbol{x}) = (\epsilon^{r_1}x_1, \epsilon^{r_2}x_2, \ldots, \epsilon^{r_n}x_n)$, where $r_i > 0$ and $\boldsymbol{x} = \begin{bmatrix} x_1 & x_2 & \ldots & x_n \end{bmatrix}^T$, if for each i, $f_i(\epsilon^{r_1}x_1, \epsilon^{r_2}x_2, \ldots, \epsilon^{r_n}x_n) = \epsilon^{d+r_i} f_i(x_1, x_2, \ldots, x_n)$ for any $\epsilon > 0$.*

Theorem 2. *[47] Suppose the vector field $\boldsymbol{f}$ is homogeneous with degree d. Then, the origin of the system $\dot{\boldsymbol{x}}(t) = \boldsymbol{f}(\boldsymbol{x}(t))$ is FTS if and only if it is asymptotically stable and $d < 0$.*

Theorem 3. *[59] The origin of the system $\dot{\boldsymbol{x}}(t) = -k\boldsymbol{x}\|\boldsymbol{x}\|^{\alpha-1}$ is GFTS for any $k > 0$ and $0 < \alpha < 1$.*

*This can be verified using $\boldsymbol{x} = \boldsymbol{u}_i - \boldsymbol{u}_{id}$ in Theorem 3.

B. Finite-time Stable State-estimator

The feedback control law (13) requires full-state information. Since only partial state is available via the system output, we make use of an FTS state-estimator inspired from [60], given by:

$$\dot{\hat{\boldsymbol{r}}}_i = \hat{\boldsymbol{u}}_i + k_{i3}(\boldsymbol{y}_i - \hat{\boldsymbol{y}}_i)\|\boldsymbol{y}_i - \hat{\boldsymbol{y}}_i\|^{\alpha_1 - 1} + \boldsymbol{w}_{av} \tag{14a}$$

$$\dot{\hat{\boldsymbol{u}}}_i = \boldsymbol{a}_i + k_{i4}(\boldsymbol{y}_i - \hat{\boldsymbol{y}}_i)\|\boldsymbol{y}_i - \hat{\boldsymbol{y}}_i\|^{\alpha_2 - 1}, \tag{14b}$$

where $\hat{\boldsymbol{y}}_i = \hat{\boldsymbol{r}}_i$ is the estimated output, $0 < \alpha_1, \alpha_2 < 1$, and $k_{i3}, k_{i4} > 0$. Define the error terms $\boldsymbol{r}_{ie} \triangleq \boldsymbol{r}_i - \hat{\boldsymbol{r}}_i = \boldsymbol{y}_i - \hat{\boldsymbol{y}}_i$ and $\boldsymbol{u}_{ie} \triangleq \boldsymbol{u}_i - \hat{\boldsymbol{u}}_i$, so that from (1) and (14), we obtain:

$$\dot{\boldsymbol{r}}_{ie} = \boldsymbol{u}_{ie} - k_{i3}\boldsymbol{r}_{ie}\|\boldsymbol{r}_{ie}\|^{\alpha_1 - 1} + \boldsymbol{w}(\boldsymbol{r}_i, t) - \boldsymbol{w}_{av} \tag{15a}$$

$$\dot{\boldsymbol{u}}_{ie} = -k_{i4}\boldsymbol{r}_{ie}\|\boldsymbol{r}_{ie}\|^{\alpha_2 - 1}. \tag{15b}$$

In order to show the finite time convergence of the estimation error, we first need the following results:

Lemma 2. *If $\boldsymbol{w}(\boldsymbol{r}_i, t) = \boldsymbol{0}$, the origin is an asymptotically stable equilibrium of the system* (15)*.*

Proof. Note that $\boldsymbol{w}(\boldsymbol{r}_i, t) = \boldsymbol{0}$ implies that there is no external disturbance and the system (15) is autonomous. Choose the candidate Lyapunov function

$$V(\boldsymbol{r}_{ie}, \boldsymbol{u}_{ie}) = \frac{k_{i4}}{1 + \alpha_2}\|\boldsymbol{r}_{ie}\|^{1+\alpha_2} + \frac{1}{2}\|\boldsymbol{u}_{ie}\|^2.$$

Taking its time derivative along the trajectories of (15), we obtain:

$$\dot{V}(\boldsymbol{r}_{ie}, \boldsymbol{u}_{ie}) = k_{i4}\|\boldsymbol{r}_{ie}\|^{\alpha_2 - 1}\boldsymbol{r}_{ie}^T(\boldsymbol{u}_{ie} - k_{i3}\boldsymbol{r}_{ie}\|\boldsymbol{r}_{ie}\|^{\alpha_1 - 1}) + \boldsymbol{u}_{ie}^T(-k_{i4}\boldsymbol{r}_{ie}\|\boldsymbol{r}_{ie}\|^{\alpha_2 - 1}) = -k_{i3}k_{i4}\|\boldsymbol{r}_{ie}\|^{\alpha_1 + \alpha_2} \leq 0.$$

Now, since $\alpha_1 + \alpha_2 > 0$, $\dot{V}(\boldsymbol{r}_{ie}, \boldsymbol{u}_{ie}) = 0$ at $\boldsymbol{r}_{ie} \equiv \boldsymbol{0}$ for any $\boldsymbol{u}_{ie}$. Using LaSalle's invariance principle, we have that the origin is the only point where the trajectories of the system (15) can identically stay. Hence, the origin is an asymptotically stable equilibrium of the system (15) when $\boldsymbol{w}(\boldsymbol{r}_i, t) = \boldsymbol{0}$. □

Lemma 3. *For $\boldsymbol{w}(\boldsymbol{r}_i, t) = \boldsymbol{0}$ and $\alpha_1 = \alpha$, $\alpha_2 = 2\alpha - 1$, where $\frac{1}{2} < \alpha < 1$, the error dynamics* (15) *is homogeneous with degree of homogeneity $d = \alpha - 1 < 0$.*

Proof. Let $r_1 = 1$ and $r_2 = \alpha$, with $\frac{1}{2} < \alpha < 1$. With these parameters, define the dilation function $\Delta_\epsilon(\boldsymbol{r}, \boldsymbol{u}) = (\epsilon\boldsymbol{r}, \epsilon^\alpha\boldsymbol{u})$. Define the right hand side of (15) as $\boldsymbol{f}^{err}(\boldsymbol{r}_{ie}, \boldsymbol{u}_{ie}) = \begin{bmatrix} f_1^{err}(\boldsymbol{r}_{ie}, \boldsymbol{u}_{ie}) & f_2^{err}(\boldsymbol{r}_{ie}, \boldsymbol{u}_{ie}) \end{bmatrix}^T$. Now, for $\boldsymbol{w}(\boldsymbol{r}_i, t) = \boldsymbol{0}$, define

$d \triangleq \alpha - 1$ so that for any $\epsilon > 0$ we obtain:

$$f_1^{err}(\epsilon^{r_1}\boldsymbol{r}_{ie}, \epsilon^{r_2}\boldsymbol{u}_{ie}) = \epsilon^{r_2}\boldsymbol{u}_e - k_{i3}\epsilon^{r_1\alpha_1}\boldsymbol{r}_{ie}\|\boldsymbol{r}_{ie}\|^{\alpha_1-1} = \epsilon^{\alpha}(\boldsymbol{u}_e - k_{i3}\boldsymbol{r}_{ie}\|\boldsymbol{r}_{ie}\|^{\alpha_1-1}) = \epsilon^{d+r_1} f_1^{err}(\epsilon^{r_1}\boldsymbol{r}_{ie}, \epsilon^{r_2}\boldsymbol{u}_{ie}),$$
$$f_2^{err}(\epsilon^{r_1}\boldsymbol{r}_{ie}, \epsilon^{r_2}\boldsymbol{u}_{ie}) = -k_{i4}\epsilon^{r_1\alpha_2}r_e\|\boldsymbol{r}_{ie}\|^{\alpha_2-1} = \epsilon^{2\alpha-1}(-k_{i4}\epsilon^{\boldsymbol{r}_1\alpha_2}r_e\|\boldsymbol{r}_{ie}\|^{\alpha_2-1}) = \epsilon^{d+r_2} f_2^{err}(\epsilon^{r_1}\boldsymbol{r}_{ie}, \epsilon^{r_2}\boldsymbol{u}_{ie}).$$

Thus, from Definition 2, the error dynamics is homogeneous with degree $d = \alpha - 1 < 0$. □

From [47, Theorem 7.1], we have that the origin is a finite-time stable equilibrium for (15) if $\boldsymbol{w}(\boldsymbol{r}_i, t) = \boldsymbol{0}$, i.e. in the absence of the disturbance. Now, we show that in the presence of the disturbance $\boldsymbol{w}(\boldsymbol{r}_i, t)$, the estimation error remains bounded:

Theorem 4. *With α_1, α_2 as per Lemma 3, the norm of the state estimation error is bounded as*

$$\left\| \begin{bmatrix} \boldsymbol{r}_{ie}(t)^T & \boldsymbol{u}_{ie}(t)^T \end{bmatrix}^T \right\| \leq \delta_{ie}(t)$$

for all $t \geq 0$, where $\delta_{ie}(t)$ is defined as

$$\delta_{ie}(t) = \begin{cases} \|\boldsymbol{u}_{ie}(0)\|, & 0 \leq t \leq T_i^{obs}; \\ l_i \delta_w^{c_i}, & t > T_i^{obs}; \end{cases} \tag{16}$$

where $l_i = (2(1-\beta))^{\frac{1-\beta}{\beta}} \|\boldsymbol{u}_{ie}(0)\| > 0$, $c_i = \frac{1-\beta}{\beta} > 1, 0 < \beta < \frac{1}{2}$, and $0 \leq T_i^{obs} < \infty$ is a finite constant.

Proof. See Appendix B. □

Remark 4. The reason for using a finite-time state-estimator instead of a Luenberger observer is that, as shown in [46], the bound on state (in our case, state-estimation error) δ_{ie} in Theorem 4 is of higher order than the bound on the disturbance δ_w ($c_i > 1$), leading to improved rejection of low-level persistent disturbances.

Next we design a robust controller using the estimated states $\hat{\boldsymbol{r}}_i, \hat{\boldsymbol{u}}_i$.

C. Observer-based Robust Controller

We first re-design the desired velocity using the estimated states as follows:

$$\hat{\boldsymbol{u}}_{id} = \hat{u}_{id}\hat{\boldsymbol{u}}_{idn} - k_{i3}\boldsymbol{r}_{ie}\|\boldsymbol{r}_{ie}\|^{\alpha_1-1} - \boldsymbol{w}_{av}, \tag{17a}$$
$$\hat{\boldsymbol{u}}_{idn} = \begin{bmatrix} \cos\hat{\gamma}_i & \sin\hat{\gamma}_i \end{bmatrix}^T, \tag{17b}$$

where $\hat{\gamma}_i \triangleq \gamma_i(\hat{\boldsymbol{r}}_i)$. Note that in the absence of actual state measurements, the vector field $\mathbf{F}_i, \hat{\gamma}_i$ and the bump function $\sigma = \sigma(\hat{d}_{ij})$, where $\hat{d}_{ij}$ is given by (21), are functions of the estimated/sensed positions. Define the set I_i as

$$I_i = \{j \in \mathcal{N}_i | \hat{J}_i < 0, d_s \leq \hat{d}_{ij} \leq R_c\}, \tag{18}$$

as the set of agents who are in the sensing range of agent i such that the agent i is moving towards them, i.e., $\hat{J}_i \triangleq \hat{\boldsymbol{r}}_{ji}^T \hat{\boldsymbol{u}}_{idn} < 0$. The new desired speed $\hat{u}_{id}$ for agent i is set as:

$$\hat{u}_{id} = \begin{cases} \frac{1}{\mu} \log\left(\left(\sum\limits_{j \in \mathcal{N}_i | \hat{d}_{ij} \leq d_s} e^{-\mu\, \hat{u}_{is|j}}\right)^{-1} + 1\right), & I_i = \emptyset \;\&\; \hat{d}_{ij} \leq d_s; \\ u_{ic}, & I_i = \emptyset \;\&\; \hat{d}_{ij} > d_s; \\ \frac{1}{\mu} \log\left(\left(\sum\limits_{j \in I_i} e^{-\mu\, \hat{u}_{i|j}}\right)^{-1} + 1\right), & I_i \neq \emptyset; \end{cases} \tag{19}$$

where $\hat{u}_{i|j}$ is defined as:

$$\hat{u}_{i|j} = u_{ic} \frac{\hat{d}_{ij} - d_s}{R_c - d_s} + \hat{u}_{is|j} \frac{R_c - \hat{d}_{ij}}{R_c - d_s}, \tag{20}$$

where d_s is defined as per Theorem 5, $u_{ic} = u_{ic}(\hat{\boldsymbol{r}}_i)$ is as per (10a) and rest of the terms in (20) are given as:

$$\hat{u}_{is|j} = \varepsilon_i \frac{\hat{\boldsymbol{r}}_{ji}^T \boldsymbol{u}_{js}^i}{\hat{\boldsymbol{r}}_{ji}^T \hat{\boldsymbol{u}}_{idn}} + (1 - \varepsilon_i) \frac{u_e d_s}{\hat{\boldsymbol{r}}_{ji}^T \hat{\boldsymbol{u}}_{idn}}, \quad 0 < \varepsilon_i < 1, \quad \hat{J}_j = \hat{\boldsymbol{r}}_{ji}^T \hat{\boldsymbol{u}}_{idn}, \quad \hat{\boldsymbol{r}}_{ji} = \hat{\boldsymbol{r}}_i - \boldsymbol{r}_{js}^i, \quad \hat{d}_{ij} = \|\hat{\boldsymbol{r}}_{ji}\|, \tag{21}$$

where $\boldsymbol{u}_{js}^i$ and $\boldsymbol{r}_{js}^i$ are the position and velocity of agent $j \in \mathcal{N}_i$ as *sensed* by agent i and u_e is defined later as per (35). Consider the dynamics (14) with an objective of tracking the velocity command $\hat{\boldsymbol{u}}_{id}$ given as per (17). We design the acceleration controller as follows:

$$\boldsymbol{a}_i = \dot{\hat{\boldsymbol{u}}}_{id} - \lambda_i \boldsymbol{u}_{ide} \|\boldsymbol{u}_{ide}\|^{\beta_2 - 1} - k_{i4} \boldsymbol{r}_{ie} \|\boldsymbol{r}_{ie}\|^{\alpha_2 - 1}, \tag{22a}$$

$$\boldsymbol{u}_{ide} = \hat{\boldsymbol{u}}_i - \hat{\boldsymbol{u}}_{id}, \tag{22b}$$

where $\lambda_i > 0, 0 < \beta_2 < 1$ and $\boldsymbol{u}_{ide}$ is the velocity error between the desired velocity $\hat{\boldsymbol{u}}_{id}$ and the velocity of the observer $\hat{\boldsymbol{u}}_i$. In the next subsections, we show that the system (1) converges to a small neighborhood of the desired goal location $\boldsymbol{r}_{gi}$, while maintaining safety.

D. Safety Analysis

First we define the estimation error parameter δ_e as

$$\delta_e \triangleq \max_{i,t} \delta_{ie}(t) = \max_i \{\boldsymbol{u}_{ie}(0), l_i \delta_w^{c_i}\}, \tag{23}$$

so that $\|\boldsymbol{r}_i(t) - \hat{\boldsymbol{r}}_i(t)\| \leq \delta_e$ and $\|\boldsymbol{u}_i(t) - \hat{\boldsymbol{u}}_i(t)\| \leq \delta_e$ for all agents i and for all time $t \geq 0$.

Theorem 5. *Assume N agents $i \in \{1, 2, \ldots, N\}$ are moving under the effect of acceleration controller* (22)*. If the safe separation of each agent i is taken as $d_s = d_m + r_e + \delta_e + \epsilon_s$, with r_e being the maximum overshoot of the position error in the transient period of the closed-loop system* (14) *given out of* (40)*, and δ_e is defined as in* (23)*, then the motion of all agents is collision free, i.e. $\|\boldsymbol{r}_i(t) - \boldsymbol{r}_j(t)\| \geq d_m$ for all $i \neq j$ and for all $t \geq 0$.*

Proof. See Appendix C. □

E. Convergence Analysis

Now we show that under the effect of the designed control law (22), the closed-loop trajectories of agent i reach the $\delta_{ie}-$neighbourhood around the goal location $\boldsymbol{r}_{gi}$ in finite time. We need the following result before we proceed with the main result.

Lemma 4. *Consider the system $\dot{\boldsymbol{x}}(t) = -k\boldsymbol{x}(t)\frac{\tanh(\|\boldsymbol{x}(t)\|)}{\|\boldsymbol{x}(t)\|}$ for some $k > 0$. Assume that $\boldsymbol{x}(0) \neq \boldsymbol{0}$. Then, for any $\epsilon > 0$, there exists a time $T_\epsilon < \infty$ such that $\|\boldsymbol{x}(t)\| \leq \epsilon$ for all $t \geq T_\epsilon$.*

Proof. See Appendix D. □

Now we are ready to state the main result for convergence.

Theorem 6. *Under the effect of control law* (22)*, the closed-loop trajectories of* (1) *for each agent i reach a δ_{ie}-neighbourhood around the goal location $\boldsymbol{r}_{gi}$ in finite time, i.e., $\exists\, T_i < \infty$, such that $\|\boldsymbol{r}_i(t) - \boldsymbol{r}_{gi}\| \leq \delta_{ie}(t)$ for all time $t \geq T_i$.*

Proof. See Appendix E. □

IV. Dynamic Obstacle Environment

Let us now consider the case when the agents, termed as class-A agents subsequently, have to navigate in an obstacle environment. We consider M dynamic obstacles $o \in \mathcal{N}_B = \{N+1, \ldots, N+M\}$ that are moving with upper-bounded linear velocity $\|\boldsymbol{u}_o\| \geq 0$. These can model agents of higher priority, adversarial agents that are non-cooperative to the motion of the class-A agents, or failed class-A agents whose motion is uncontrollable. In what follows, we refer to this class of dynamic obstacles as class-B agents [30]. We need the following assumptions in order to guarantee safety of the system in the presence of dynamic obstacles.

Assumption 4. *Class-B agents are assumed to have circular shape with same size. The velocity of the class-B agents are bounded as* $\|\boldsymbol{u}_o\| \leq u_o$ *with* $0 \leq u_o < \infty$.

Assumption 5. *For any two class-B agents* o_1, o_2*, the inter-agent distance is* $\|\boldsymbol{r}_{o_1}(t) - \boldsymbol{r}_{o_2}(t)\| > 2d_s$ *for almost all* $t \geq 0$*, i.e., any two class-B agents are not very close to each other at all times. Furthermore, for all class-B agents* o *and for all* $i \in \{1, \cdots, N\}$*,* $\|\boldsymbol{r}_o(t) - \boldsymbol{r}_{gi}\| \geq R_c + \delta_e$ *for almost all* $t \geq 0$*, i.e. the dynamic obstacles do not remain very close to the goal locations of the class-A agents at all times.*

Remark 5. Assumption 5 is needed to guarantee that no class-A agent can become permanently occluded by a group of class-B agents and that they are not in conflict with class-B agents at their goal locations. Note that this is a sufficient condition to eliminate this situation. It might happen that even if the class-B agents are very close to each other, the class-A agents are able to skip through and reach their goal location (see Section V for details).

Note that unlike [30], we do not consider any communication between agents. The class-A agents do not even need to know whether their neighboring agents are class-A or class-B. We are now ready to propose the coordination protocol for the multi-agent system in the presence of dynamic obstacles.

A. Safe Velocity Design

The desired linear velocity $\hat{\boldsymbol{u}}_{id}$ of each agent i is defined as per (17) where the modified $\hat{u}_{id}$ is

$$\hat{u}_{id} = \begin{cases} -\frac{1}{\mu}\log\left(\sum\limits_{j\in\mathcal{N}_i|\hat{d}_{ij}\leq d_s} e^{-\mu\,\hat{u}^1_{is|j}}\right) & \hat{d}_{ij} \leq d_s, \\ -\frac{1}{\mu}\log\left(\sum\limits_{j\in\mathcal{N}_i} e^{-\mu\,\hat{u}^1_{i|j}}\right), & d_s \leq \hat{d}_{ij} \leq R_c, \\ u_{ic}, & \hat{d}_{ij} > R_c; \end{cases} \quad , \tag{24}$$

where $\hat{u}^1_{i|j}$ is

$$\hat{u}^1_{i|j} = \hat{u}_{ic}\frac{\hat{d}_{ij} - d_s}{R_c - d_s} + \hat{u}^1_{is|j}\frac{R_c - \hat{d}_{ij}}{R_c - d_s} \tag{25}$$

$\hat{u}^1_{is|j}$ is

$$\hat{u}^1_{is|j} = \begin{cases} (1+\varepsilon_i)\frac{\hat{\boldsymbol{r}}^T_{ji}\boldsymbol{u}^i_{js}}{\hat{\boldsymbol{r}}^T_{ji}\hat{\boldsymbol{u}}_{idn}}, & \hat{J}_j > 0, \\ \varepsilon_i\frac{\hat{\boldsymbol{r}}^T_{ji}\boldsymbol{u}^i_{js}}{\hat{\boldsymbol{r}}^T_{ji}\hat{\boldsymbol{u}}_{idn}}, & \hat{J}_j \leq 0; \end{cases} \quad , \tag{26}$$

$\hat{J}_j = \hat{\boldsymbol{r}}^T_{ji}\hat{\boldsymbol{u}}^i_{js}$, and rest of the terms such as $\varepsilon_i, \hat{d}_{ij}$ are given as in (21).

Remark 6. *Note that the expression in* (24) *is different from* (19) *since, in the latter case, we restrict the desired $\hat{u}_{id}$ to be always positive. In* (24)*, we remove the* (+1) *term in the argument of logarithm, allowing $\hat{u}_{id}$ to take negative values as well.*

B. Safety Analysis in the presence of Dynamic Obstacles

With this definition of the desired velocity $\hat{\boldsymbol{u}}_{id}$ with $\hat{u}_{id}$ given by (24), we can state the following result:

Theorem 7. *Consider N class-A agents $i \in \{1, \ldots, N\}$ assigned to move to goal locations $\boldsymbol{r}_{gi}$, and M class-B agents $o \in \{N+1, \ldots, N+M\}$ serving as dynamic obstacles satisfying Assumption 4-5. Then, with d_s given as per Theorem 5, under the coordination protocol* (22) *with desired velocity defined as in* (17) *and $\hat{u}_{id}$ given as per* (24)*, each class-A agent maintains safe distance d_m with other agents.*

Proof. As per the analysis in the proof of Theorem 5, we obtain that for any $j \in \mathcal{N}_i$, $\hat{d}_{ij} = \|\hat{\boldsymbol{r}}_i - \hat{\boldsymbol{r}}_j\| \geq d_s \implies \|\boldsymbol{r}_i - \boldsymbol{r}_j\| \geq d_m$. So, it is sufficient to prove that $\hat{d}_{ij} \geq d_s$ for all time t and for all $i \neq j$, i in class A, or equivalently, to prove that at $\hat{d}_{ij} = d_s$, the time derivative $\dot{\hat{d}}_{ij} \geq 0$. According to the control law (24), the agent i adjusts its linear velocity u_i so that it avoids colliding with the neighbor $j \in \mathcal{N}_i$ whose motion maximizes the rate of change of relative distance d_{ij}. Consider that $\hat{J}_j = \hat{\boldsymbol{r}}_{ji}^T \hat{\boldsymbol{u}}_{js}^i > 0$, i.e., the class-B agent o is moving towards the agent i. The time derivative of the inter-agent distance, evaluated at $\hat{d}_{ij} = d_s$, given by (33) under the closed-loop protocol (24) reads

$$\dot{\hat{d}}_{ij} = \frac{\hat{u}_{id}\, \hat{\boldsymbol{r}}_{ji}^T \hat{\boldsymbol{u}}_{idn} - \hat{\boldsymbol{r}}_{ji}^T \hat{\boldsymbol{u}}_{js}^i}{\hat{d}_{ij}} = \frac{(1+\varepsilon_i)\hat{\boldsymbol{r}}_{ji}^T \boldsymbol{u}_{js}^i - \hat{\boldsymbol{r}}_{ji}^T \hat{\boldsymbol{u}}_{js}^i}{\hat{d}_{ij}} = \frac{\varepsilon_i \hat{\boldsymbol{r}}_{ji}^T \boldsymbol{u}_{os}^i}{\hat{d}_{ij}} \geq 0.$$

Similarly, when $\hat{J}_j = \hat{\boldsymbol{r}}_{ji}^T \hat{\boldsymbol{u}}_{js}^i \leq 0$, i.e. the agent j is moving away from the agent i, the time derivative of the inter-agent distance at $\hat{d}_{ij} = d_s$ reads

$$\dot{\hat{d}}_{ij} = \frac{\hat{u}_{id}\, \hat{\boldsymbol{r}}_{ji}^T \hat{\boldsymbol{u}}_{idn} - \hat{\boldsymbol{r}}_{ji}^T \hat{\boldsymbol{u}}_{js}^i}{\hat{d}_{ij}} = \frac{\varepsilon_i \hat{\boldsymbol{r}}_{ji}^T \boldsymbol{u}_{js} - \hat{\boldsymbol{r}}_{ji}^T \hat{\boldsymbol{u}}_{js}^i}{\hat{d}_{ij}} = \frac{(\varepsilon_i - 1)\hat{\boldsymbol{r}}_{ji}^T \boldsymbol{u}_{js}^i}{\hat{d}_{ij}} \geq 0.$$

Note that the last inequality is true since $0 < \varepsilon_i < 1$. Hence, every agent i maintains safe distance from its class-B neighbors. This shows that in all possible scenarios, each class-A agent maintains safe distance from all the other agents. □

C. Convergence Analysis

Theorem 8. *Under the effect of coordination protocol* (22) *with desired velocity $\hat{\boldsymbol{u}}_{id}$ defined as in* (17) *and $\hat{u}_{id}$ given as per* (24)*, the closed-loop trajectories* (1) *of each class-A agent i reach a δ_{ie}-neighborhood around the goal location $\boldsymbol{r}_{gi}$ in finite time, i.e., $\exists\, T_i < \infty$, such that $\|\boldsymbol{r}_i(t) - \boldsymbol{r}_{gi}\| \leq \delta_{ie}(t)$ for all time $t \geq T_i$.*

Proof. According to the Assumption 5, there are no two class-B agents whose distance is less than $2d_s$ for all times,

which implies that there will always be space between the two obstacles from where the class-A agent can pass through. The rest of the proof directly follows from Theorem 6. Also, since the class-B agents are not always near the goal locations $\boldsymbol{r}_{gi}$ (Assumption 5), once the class-A agent i reaches its goal location, it can stay there. □

Remark 7. *While as per Lemma 1, there would be no deadlocks in the motion of the agents, it is still possible that there are livelocks. Livelock occurs when periodic motions are executed by the agents, that may be induced by periodic motion of class-B agents or under certain control gains, direction of the wind, and the set of initial and goal locations for the class-A agents. Excluding the livelocks is a rather difficult problem, is out of scope of the current work and is left as a problem for future investigation.*

Hence, we showed that in the presence of moving obstacles, or class-B agents, the class-A agents would be able to reach very close to the desired goal location while maintaining safety. Next we present a few simulation results to show the efficacy of the proposed control design.

V. Simulations

A. Simulation Parameters

We consider five scenarios: the first three scenarios involve $N = 46$ agents out of which 20 are class-B agents and 26 are class-A agents, the fourth scenario involves 3 class-A and 3 class-B agents, and the fifth scenario includes $N = 48$ class-A agents that are assigned to move towards goal locations while avoiding collisions. In Figure 2, class-A agents are colored blue and the class-B agents are colored red. The goal locations are selected sufficiently far apart so that the agents' sensing regions do not overlap when agents lie on their goal locations (i.e., $\|\boldsymbol{r}_{gi} - \boldsymbol{r}_{gj}\| > R_c$ for $i \neq j$). The simulation parameters for all the five scenarios are listed below:

- $d_m = 4m$, $\epsilon_s = 5$, $\delta_e = 15$, $d_s = 29\ m$ and $R_c = 3.5d_s$. Define $\Delta_e = \max_i\{l_i\delta_w^{c_i}\}$, so that from Theorem 8, we have $\|\boldsymbol{r}_{ie}\| \leq \Delta_e$ for all times $t \geq \max_i T_i$. In our case, $\Delta_e = 0.8824\ m$.
- $\boldsymbol{w}_{av} = [5.86, 2.96]^T\ m/sec$ and $\delta_w = 1.92\ m/sec$
- $\varepsilon_i = 0.01$, $k_{i1} = 5$, $k_{i3} = 0.8538$, $k_{i4} = 0.3149$, $\alpha_r = 0.9, R_1 = 0.4017m, \alpha_1 = 0.9$ and $\alpha_2 = 0.8$.

Figure 1 shows the spatial variation of the wind speed used as the external disturbance in the simulations. The the wind speed at each $x - y$ location is plotted. The figure shows the variation of the wind speed in the $x - y$ plane in the domain $[-100, 100] \times [-100, 100]$. We used the following formulation to scale up the domain of the disturbance:

$$\boldsymbol{w}(x \pm 200, y \pm 200, t) = \boldsymbol{w}(x, y, t) \tag{27}$$

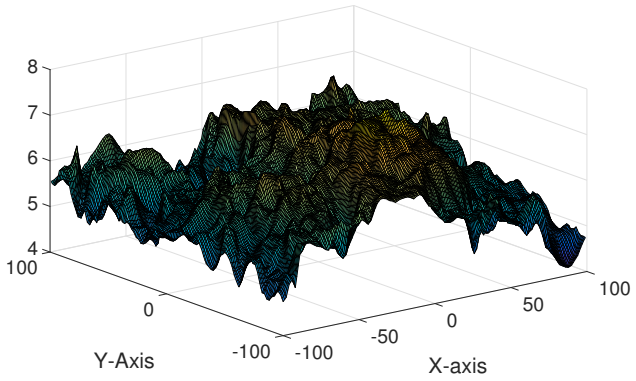

Figure 1 The wind profile used as external disturbance.

We choose the goal locations such that they form the characters UM for the aesthetic appeal of the simulations. In Figure 2, the initial positions of the agents are marked by diamonds: blue diamonds are the initial positions of class-A agents and red diamonds are those of class-B agents. In the first scenario, class-B agents are moving outwards and class-A agents are moving inwards. The black ellipse is used to denote the agents that are moving in the same direction with arrows representing their direction of motion. In Scenario 2, the class-B agents (red-diamonds) starts in V-formation as represented by the black-lines.

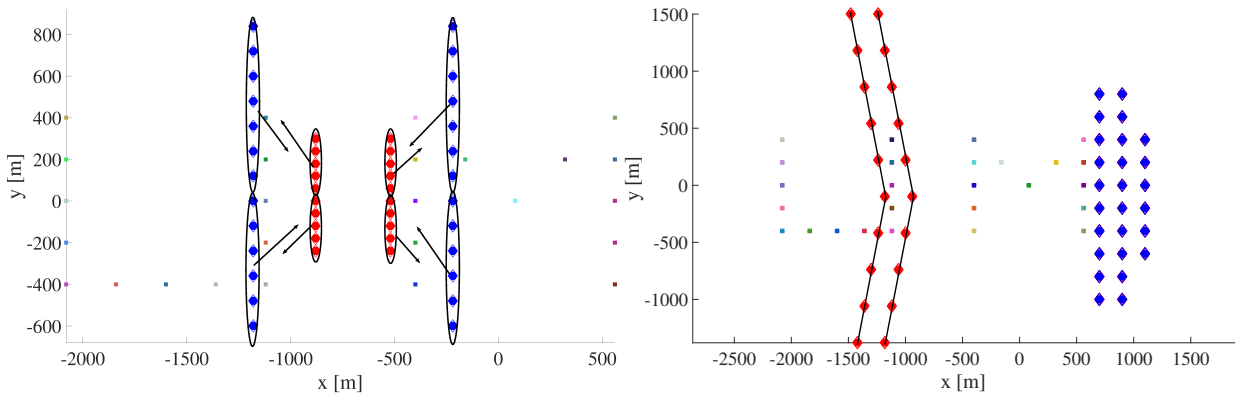

Figure 2 Initial configuration of Scenario 1 and 2.

We present five simulation scenarios. The simulation videos for all the five scenarios can be found at the link `https://www.dropbox.com/s/hu2beebxybqo20y/AIAA_JGCD_Sim.avi?dl=0`. In the first two scenarios, the class-B agents are such that the Assumption 5 is satisfied while in scenario 3, the motion of class-B agents is chosen such that Assumption 5 is not satisfied. In brief:

- In first scenario, the class-B agents start in-between the class-A agents and move outwards, while class-A agents move inwards. The set of initial locations, target locations and initial directions of movement in given in the Figure 2. This scenario shows how effectively class-A agents can avoid collisions with class-B agents. Furthermore, we assume that the wind disturbance in this case varies only with $\boldsymbol{r}$ and is constant in t, i.e. $\boldsymbol{w} = \boldsymbol{w}(\boldsymbol{r})$.

- In second scenario, the class-B agents come as a swarm in the V-formation towards the class-A agents. This scenario shows how class-A agents can avoid collisions with other class-A agents and class-B agents all together. In this case, we allow the wind disturbance to vary both in space and time, i.e. $\boldsymbol{w} = \boldsymbol{w}(\boldsymbol{r}, t)$. We discuss the difference in the results in the first two scenarios arising because of the difference in assumptions on the wind disturbance.

- In third scenario, Assumption 5 is allowed to be violated, i.e. the class-B agents move very closely to each other. In this case, as can be seen in Figure 8, we observe that the class-A agent become occluded by the formation of class-B agents and do not reach their desired locations. But, after some time, it is observed that some of the class-A agents manage to escape through; see Figure 10 and Section VI. In the forth scenario with 3 class-A and 3 class-B agents, we allow Assumption 5 to violate; see Figure 11.

- In the fifth scenario, we consider 48 class-A agents with initial and goal locations chosen on two concentric circles. Figure 12 shows the initial configuration of the agents and their desired goal locations, while Figure 13 and 14 show the simulation snapshots at various time instants.

Figures 3, 5 and 15 show the performance of the presented protocol both in terms of safety and convergence. In all the figures, it can be seen that class-A agents are able to maintain the safe distance d_m with all the other agents (both class-A and class-B agents). Also, it can be seen that the class-A agents reach to a much smaller neighborhood of their desired goal locations (i.e. their final distance from their goal location $\|\boldsymbol{r}_i - \boldsymbol{r}_{gi}\|$) than the theoretical (conservative) bound given as per Theorem 8.

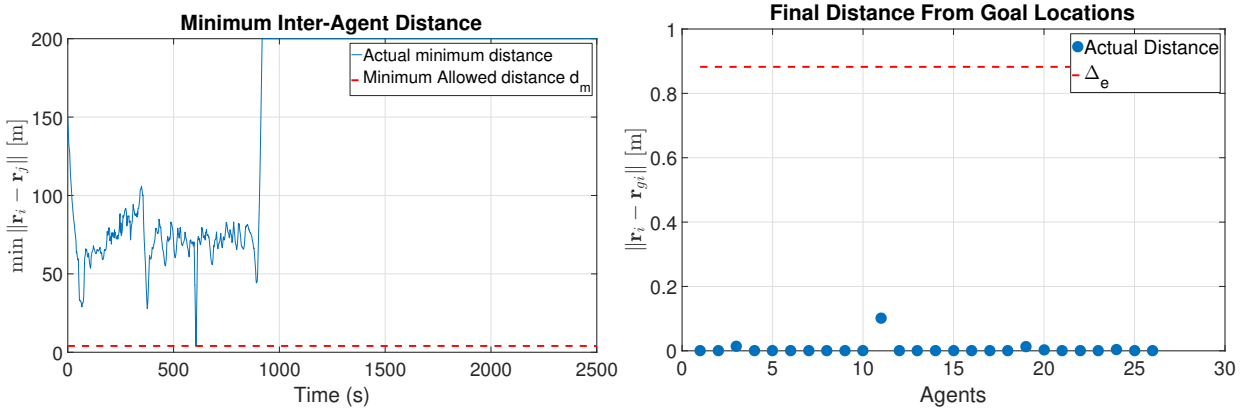

Figure 3 Scenario 1: (Safety) Minimum inter-agent distance and (Convergence) Final distance from the goal.

Note that for the observer dynamics (15), the equilibrium point is $\boldsymbol{r}^*_{ie}(t) = 0$ and $\boldsymbol{u}^*_{ie}(t) = -(\boldsymbol{w}(\boldsymbol{r}_i, t) - \boldsymbol{w}_{av})$. Since this equilibrium point varies both in space and time and we do not assume anything about the time derivative of the disturbance $\boldsymbol{w}(\boldsymbol{r}_i, t)$, we cannot prove that the system (15) would actually stay at this time varying equilibrium. As can be seen in the Figures 4, the error $\|\boldsymbol{r}_{ie}\|$ is close to 0 while $\|\boldsymbol{u}_{ie}(t)\|$ is close to $\|\boldsymbol{w}(\boldsymbol{r}_{gi}, t) - \boldsymbol{w}_{av}\|$ under the assumption

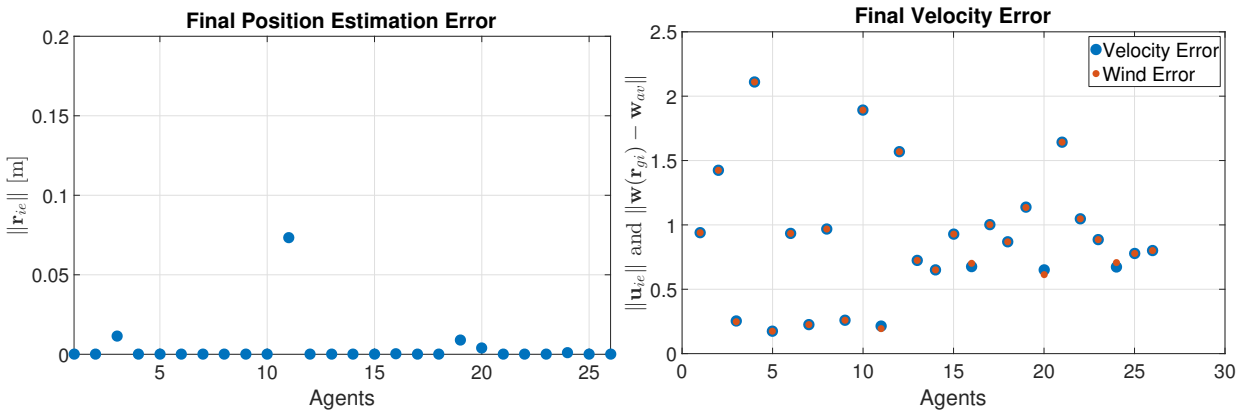

Figure 4 Scenario 1: Final position error $\|r_{ie}\|$, velocity estimation error $\|u_{ie}\|$ and $\|w(r_{gi},t) - w_{av}\|$

that $w(r_i,t)$ does not vary with time. In the case when the wind is indeed a function of time, we can see from Figure 6 that while the final estimation error is still very small, the velocity error does not converge to the actual wind error.

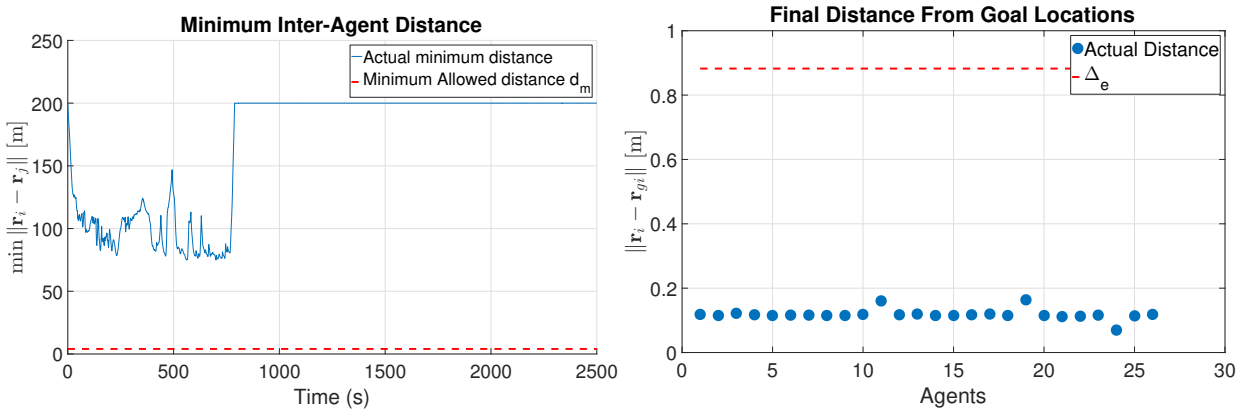

Figure 5 Scenario 2: (Safety) Minimum inter-agent distance and (Convergence) Final distance from the goal.

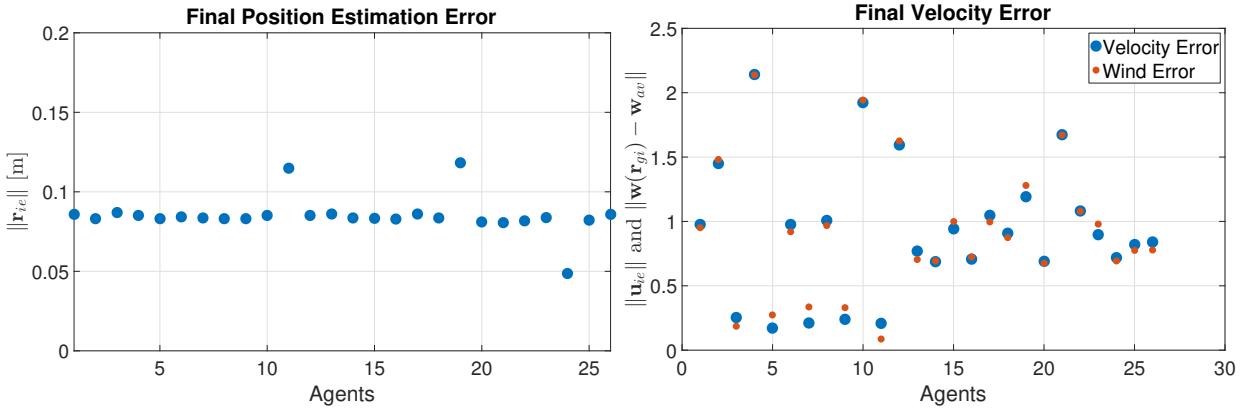

Figure 6 Scenario 2: Final position error $\|r_{ie}\|$, velocity estimation error $\|u_{ie}\|$ and the error term $\|w(r_{gi},t) - w_{av}\|$

Figure 7 shows the norm of the accelerations and the velocities of one of the class-A agents. Once the class-A agent

reaches its goal location, its velocity becomes constant, equal and opposite of the wind disturbance at the location and the acceleration becomes zero. The commanded acceleration and the velocity are noisy because of the disturbance $\boldsymbol{w}$ and the sensing uncertainties.

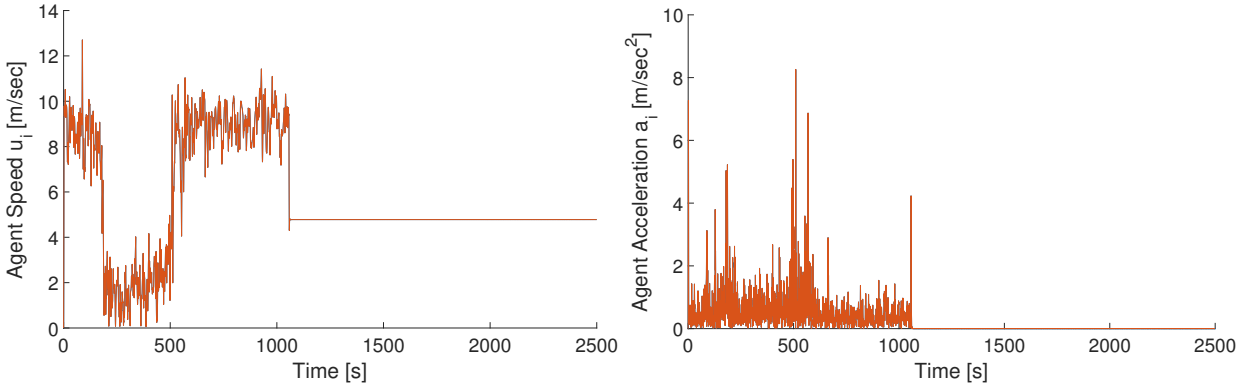

Figure 7 Magnitude of velocity and acceleration of a class-A agent.

In Figures 10-12 and Figures 14-16, the trails show the path traced by the agents in the last 60 seconds. The class-A agents are colored blue while the class-B agents are colored red. Figure 8 and 9 show the snapshots of the simulation when a few of the class-A agents get trapped in between the formation of class-B agents. Figure 10 shows how one of the class-A agents manages to escape from the formation and moves towards its goal location. This shows that even if Assumption 5 is violated, the class-A agents can still resolve the conflicts with class-B agents and reach their goal locations. To see the resulting motion of the class-A agents, the reader is requested to see the video at the link provided in the beginning of the Section V. For the sake of demonstration, we present a smaller simulation scenario with 3 class-A and 3 class-B agents in Figure 11 for the case when Assumption 5 is violated. The traces show the paths of the agents for last 150 seconds. We can see that the class-B agents are able to trap the class-A agents.

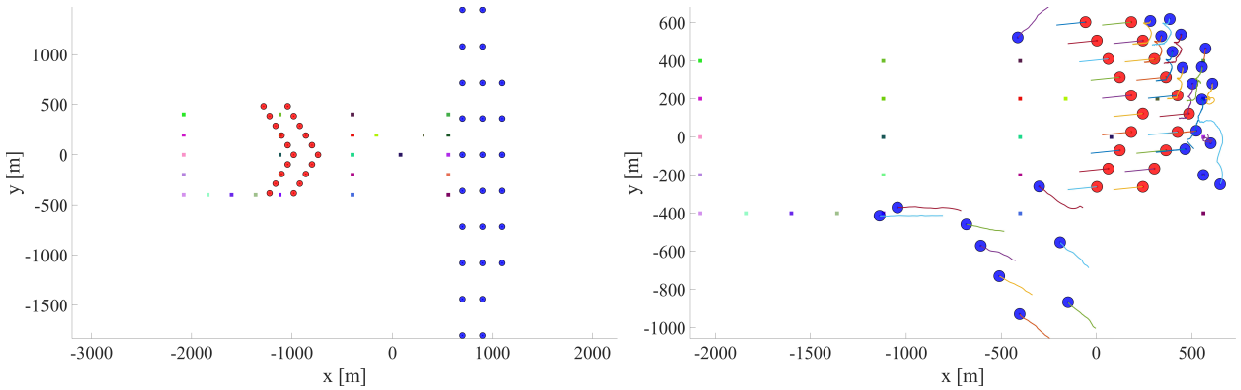

Figure 8 Scenario 3: violation of Assumption 5. Dynamic obstacles come in a V-formation: snapshots at $T = 0$ and $T = 280$ sec. The trails show the paths of the agents for last 60 sec.

In the last scenario, we simulated 48 class-A agents, and chose the initial and final locations symmetrically around

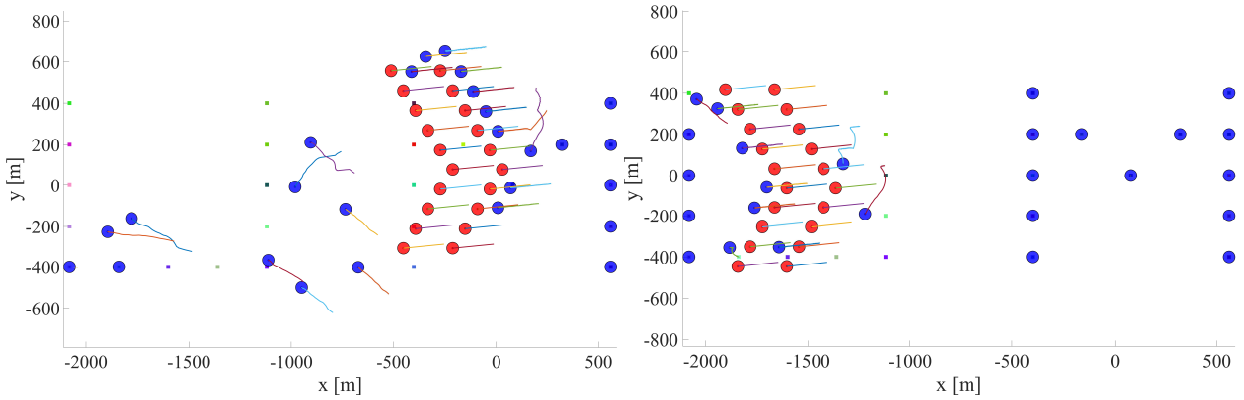

Figure 9 Scenario 3: herding of class-A agents. The class-A agents have become occluded and herded by the formation of class-B agents: snapshots at $T = 420$ and $T = 700$ sec.

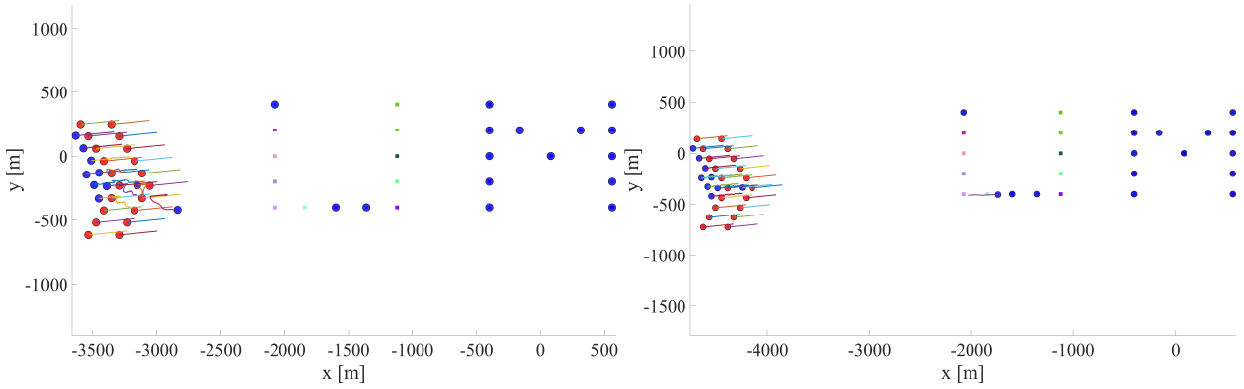

Figure 10 Scenario-3: After some time, one of the class-A agents is able to escape the occlusion caused by the motion of class-B agents: snapshots at $T = 1120$ and $T = 1260$ sec.

concentric circles such that all the agents meet in the center. Figure 12 shows the initial and the goal locations, and the snapshots at different time instants of the agents in Scenario 5. Figure 13 and 14 show the snapshots of the simulation of Scenario 5 at various time instants while Figure 15 shows the minimum inter-agent distance and their final distance from their respective goal locations. It is clear that the agents are able to resolve all the conflicts and reach their goal locations in finite time.

VI. Discussions

As demonstrated via various simulation scenarios, our proposed protocol can de-conflict large number of agents while maintaining safety and guaranteed convergence to the neighborhood of the desired goal location in the presence of unknown state-disturbances. The main strength of the proposed approach is the scalability with the number of agents and ability to counteract a class of state-disturbance and sensing uncertainties. One of the main drawbacks of the presented work is the assumption on the motion of the dynamic obstacles. It is important to note that Assumption 5 is a sufficient condition to avoid the herding of the class-A agents by a formation of class-B agents. Furthermore, it is

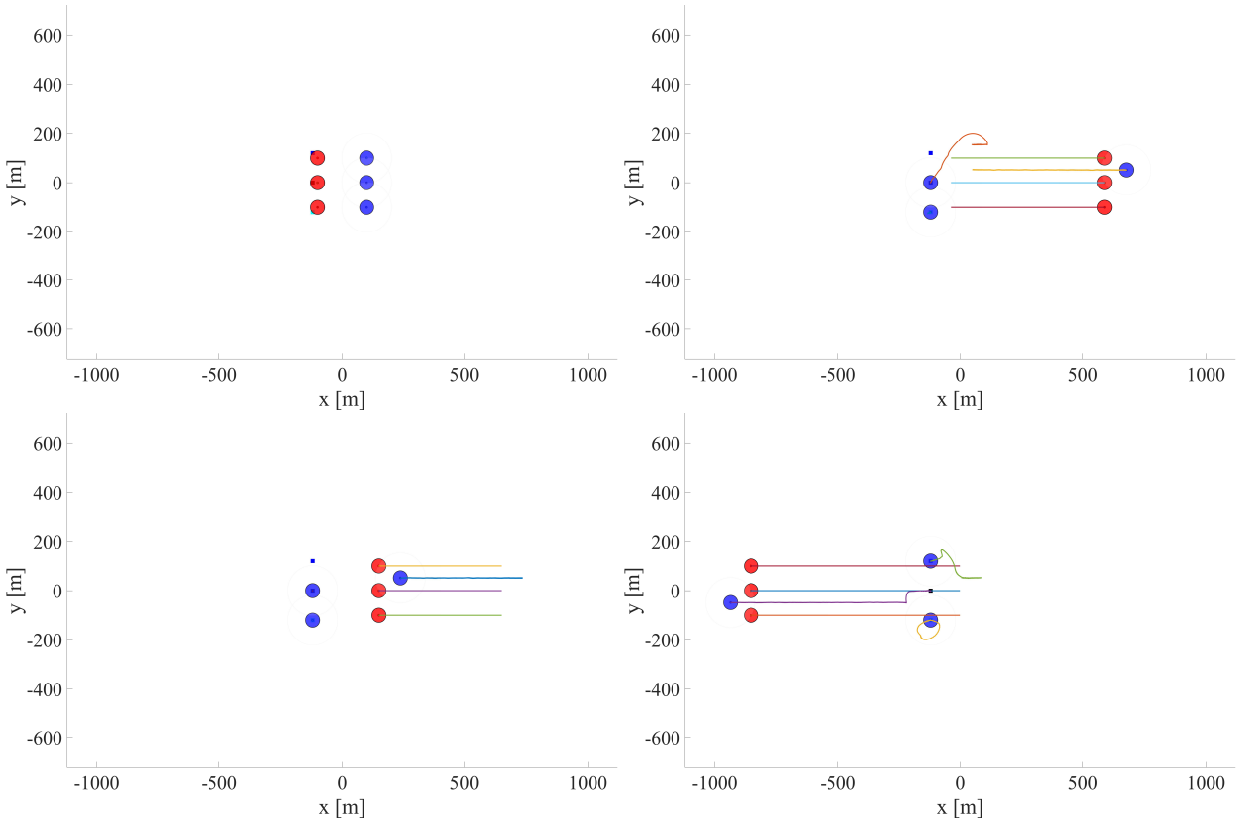

Figure 11 3 agents Scenario: Herding of class-A agents. The class-A agents have become occluded and herded by the formation of class-B agents: snapshots at $T = 0, 200, 400, 600$ sec. Trails show the paths traced by agents in last 150 seconds.

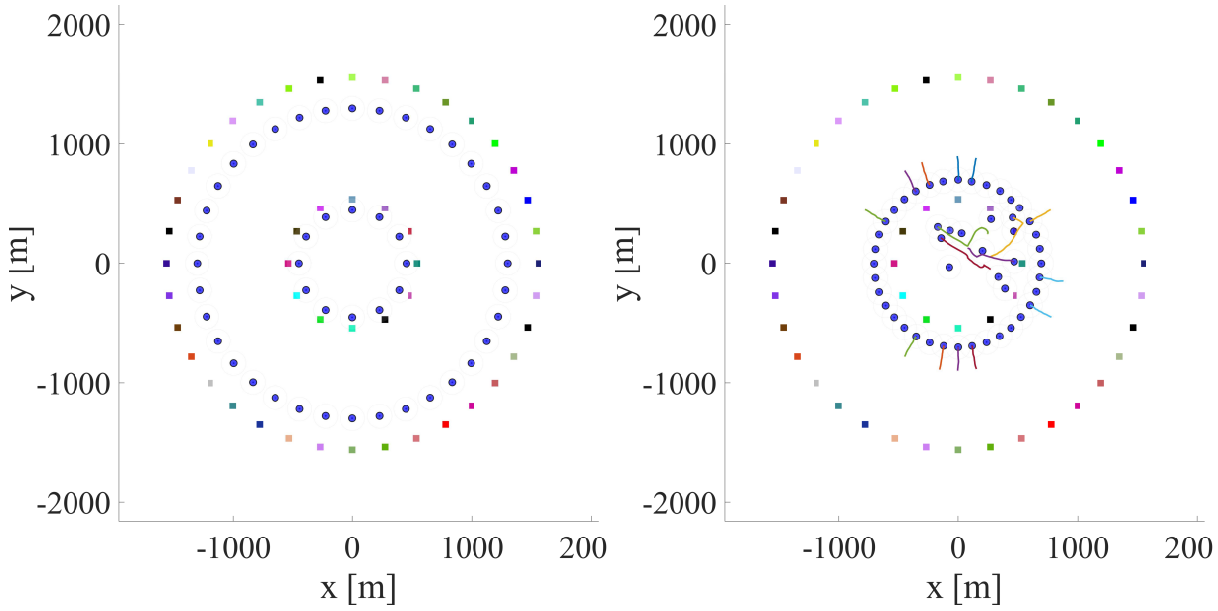

Figure 12 Scenario-5: Initial and goal locations of the 48 agents: snapshots at $T = 0$ and $T = 120$ sec.

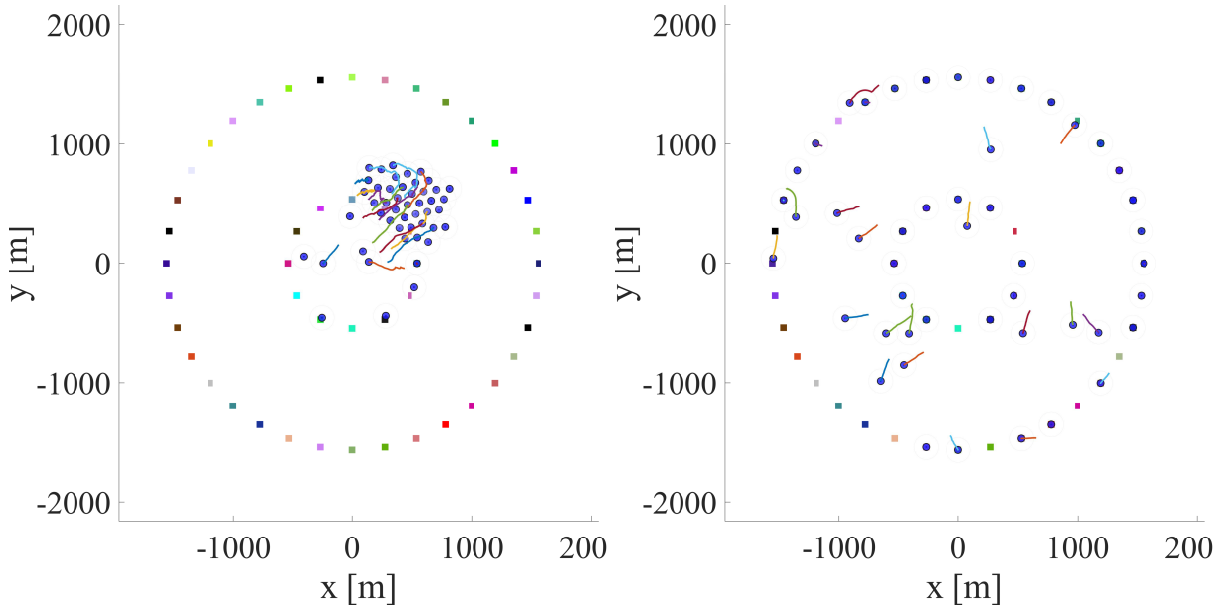

Figure 13 Scenario-5: All class-A agents come very close to each other: snapshots at $T = 240$ and $T = 480$ sec.

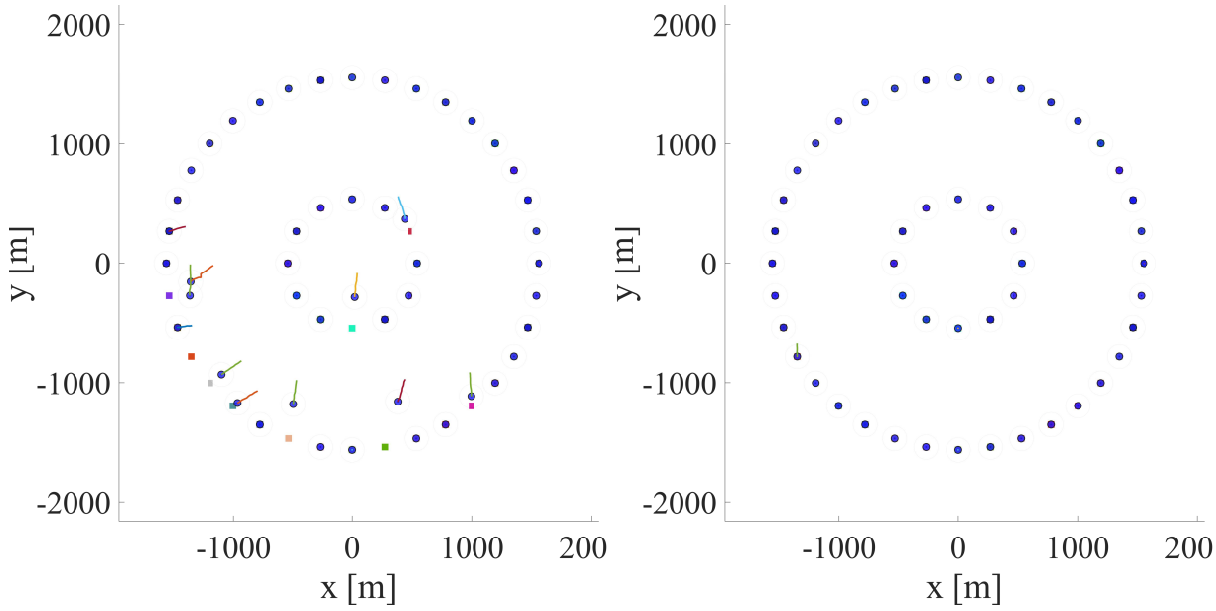

Figure 14 Scenario-5: Agents are able to resolve conflicts and reach their goal locations: snapshots at $T = 600$ and $T = 720$ sec.

required that the class-B agents do not hover around the goal location of the class-A agents so that there is no conflict once the class-A agents reach their respective goal locations. As demonstrated in Scenario 3, even if this condition fails to hold, the class-A agents can still reach their goal locations. This outcome is due to the fact that the external disturbance $\boldsymbol{w}$ and the sensing uncertainty in the positions of the neighboring agents can result into a vector field taking the class-A agents through the narrow gap between the class-B agents while maintaining safety.

One of the directions for the future work is identification of the non-cooperative neighbors. Once a class-A agent

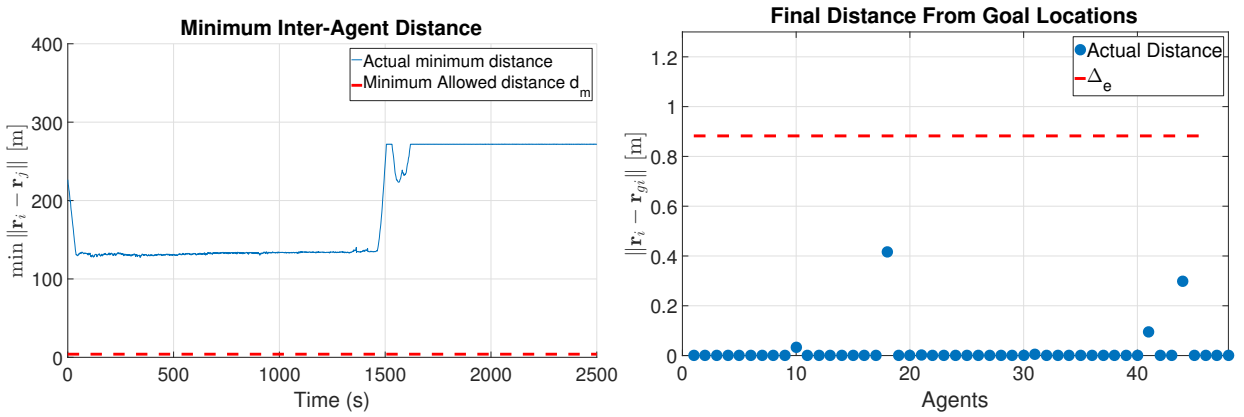

Figure 15 Scenario-4: (Safety) Minimum inter-agent distance and (Convergence) Final distance from the goal.

identifies a dynamic obstacle, it can use the knowledge of the upper bound on the velocity of the obstacle to avoid the herding.

VII. Conclusion

We present a robust distributed estimation and control scheme to generate collision-free trajectories for multiple agents in the presence of dynamic obstacles, and unmatched state disturbances standing for wind effects. We prove that under the adopted disturbance (dynamic obstacle and wind) modeling and assumptions, the safety and convergence of the system can be guaranteed. We design a finite-time observer and a finite-time feedback controller, and prove that the closed-trajectories of the each agent converge to a δ-neighborhood of their respective goal locations in a finite time, where δ depends upon the external disturbances acting on the system. Our proposed method, being completely distributed with analytical expressions for the observer and control laws, is scalable with the number of agents. We present the efficacy of the control design via various simulation scenarios. Future work includes investigating methods for identification of non-cooperative agents and consideration of more general class of obstacles, e.g. walls, buildings, for applications in urban environment.

Appendix

A. Proof of Lemma 1

Proof. It is sufficient to prove that if displaced along γ_i when $\mathbf{F}_i = \mathbf{0}$, the resulting field at the displaced location drives the agent away from the point of deadlock. More specifically, if $\boldsymbol{r}_i$ is the position of the agent i such that $\mathbf{F}_i(\boldsymbol{r}_i) = \mathbf{0}$, then after displacement $\delta\boldsymbol{r}_i$ along the direction γ_i, we need $\mathbf{F}_i(\boldsymbol{r}_i + \delta\boldsymbol{r}_i) \neq \mathbf{0}$ and that $\angle\mathbf{F}_i(\boldsymbol{r}_i + \delta\boldsymbol{r}_i) = \gamma_i$, which results in agent i moving away from $\boldsymbol{r}_i$.

Let us consider a scenario with K agents, where $2 \leq K \leq N$, such that for each agent i among these K agents, located at $\boldsymbol{r}_i$, the resulting vector fields $\mathbf{F}_i(\boldsymbol{r}_i) = \mathbf{0}$; an example is shown in Figure 16. We can assume that for all $j \in \mathcal{N}_i$

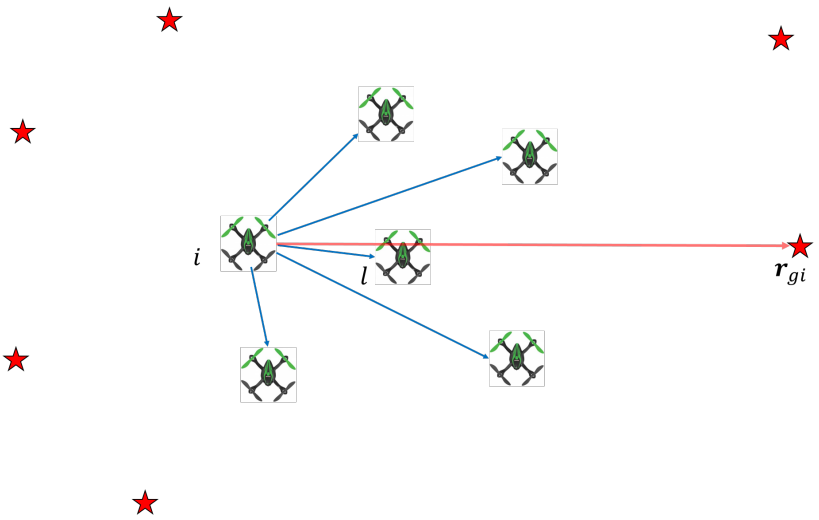

Figure 16 A scenario with 6 agents located such that their resultant vector fields are 0. Blue arrows represent the vectors $r_j - r_i$ for each $j \in \mathcal{N}_i$ and red arror represents the vector $r_{gi} - r_i$.

we have $\mathbf{F}_j = \mathbf{0}$. If this is not true for some j, then this agent would have a non-zero vector field along which it moves with a non-zero speed and, hence, it would either go out of the sensing region of the agent i in a finite time, or would reach a location $\boldsymbol{r}_j$ such that $\mathbf{F}_j(\boldsymbol{r}_j) = \mathbf{0}$.

We denote the effect of the rest of the $K-1$ agents on the agent i as a cumulative repulsive field $\mathbf{F}_{rep}$, so that we have:

$$\mathbf{F}_i = \mathbf{F}_{rep} + \prod_j (1 - \sigma_{ij})\mathbf{F}_{gi} = \mathbf{0}. \tag{28}$$

Let $\bar{\sigma} = \prod_j (1 - \sigma_{ij})$. As per the Figure 16, there is at least one agent i such that $(\boldsymbol{r}_{gi} - \boldsymbol{r}_i)^T(\boldsymbol{r}_j - \boldsymbol{r}_i) \geq 0$ for all $j \in \mathcal{N}_i$ and at least one $l \in \mathcal{N}_i$ such that $(\boldsymbol{r}_{gi} - \boldsymbol{r}_i)^T(\boldsymbol{r}_l - \boldsymbol{r}_i) > 0$. This implies that $\mathbf{F}_{gi}^T\mathbf{F}_{il} < 0$ for at least one $l \in \mathcal{N}_i$ (or, equivalently, $\mathbf{F}_{gi}^T\mathbf{F}_{rep} < 0$), since $\mathbf{F}_{il}$ acts along $-(\boldsymbol{r}_l - \boldsymbol{r}_i)$. Using this, from (28), we have:

$$\mathbf{F}_{gi}^T\mathbf{F}_i = \mathbf{F}_{gi}^T\mathbf{F}_{rep} + \bar{\sigma}\|\mathbf{F}_{gi}\|^2 = 0. \tag{29}$$

Since $\mathbf{F}_{gi}^T\mathbf{F}_{rep} < 0$, for (29) to hold, we need $\bar{\sigma} > 0$. Define an auxiliary agent o located at a location $\boldsymbol{r}_o$ to model the effect of the accumulated repulsive forces on the agent i. Let the repulsive field of agent o on agent i be given by $\mathbf{F}_{io} = \frac{\mathbf{F}_{rep}}{\bar{\sigma}}$ and $\boldsymbol{r}_o$ is such that it satisfies $\frac{\boldsymbol{r}_i - \boldsymbol{r}_o}{\|\boldsymbol{r}_i - \boldsymbol{r}_o\|} = \frac{\mathbf{F}_{rep}}{\bar{\sigma}}$, so that we have:

$$\mathbf{F}_i(\boldsymbol{r}_i) = \mathbf{F}_{io} + \mathbf{F}_{gi} = \mathbf{0}. \tag{30}$$

The equation (30) depicts a two-agent scenario consisting of agents i and o, such that $\mathbf{F}_l(\boldsymbol{r}_l) = \mathbf{0}$ for $l \in \{i, o\}$ (see

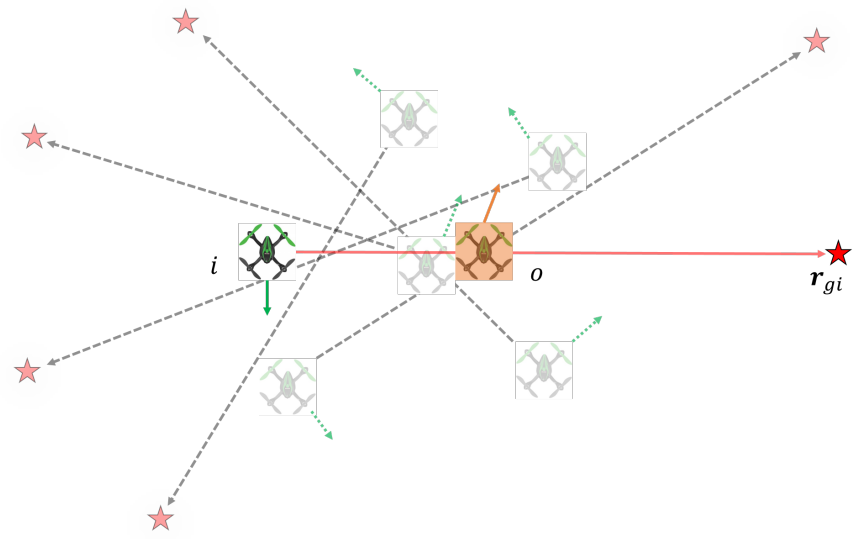

Figure 17 Motion of the agents along γ_i^0: Gray, dotted arrows show the line joining an agent and its goal location and green arrows show the instantaneous direction of motion of the agents along their respective γ_i^0. The agent shown in orange is the *virtual* agent o located at r_o, with its resultant direction of motion given by the orange arrow.

Figure 17). Since the direction of the motion of the agent i along γ_i^0 is perpendicular to the vector $\boldsymbol{r}_i - \boldsymbol{r}_{gi}$, denote it by the unit vector $(\boldsymbol{r}_i - \boldsymbol{r}_{gi})^{\perp}$. Hence, the displacement vector for agent i at the location $\boldsymbol{r}_i$ is given by $\delta\boldsymbol{r}_i = \delta_0(\boldsymbol{r}_i - \boldsymbol{r}_{gi})^{\perp}$, where $\delta_0 > 0$ denotes the infinitesimal length. Note that the resultant motion of the auxiliary agent o may or may not be perpendicular to $\boldsymbol{r}_i - \boldsymbol{r}_{gi}$, since it would depend upon the locations of the rest of the $K-1$ agents. Denote by $\delta\boldsymbol{r}_o$ the displacement of the auxiliary agent o, so that it satisfies:

$$\delta\boldsymbol{r}_o = -\delta_1(\boldsymbol{r}_i - \boldsymbol{r}_{gi})^{\perp} + \delta_2(\boldsymbol{r}_i - \boldsymbol{r}_{gi})^{\parallel}, \tag{31}$$

where $(\boldsymbol{r}_i - \boldsymbol{r}_{gi})^{\parallel}$ denotes a unit vector along $(\boldsymbol{r}_i - \boldsymbol{r}_{gi})$, $\delta_1 > 0$ and δ_2 can be either positive or negative, because the motion of the agent o would be in the opposite direction as agent i along the vector $(\boldsymbol{r}_i - \boldsymbol{r}_{gi})^{\perp}$, but can be in the either directions along the vector $(\boldsymbol{r}_i - \boldsymbol{r}_{gi})^{\parallel}$. Using this, we can express the vector field $\mathbf{F}_i$ after this infinitesimal displacement

as:

$$\begin{aligned}
\mathbf{F}_i(\boldsymbol{r}_i+\delta\boldsymbol{r}_i,\boldsymbol{r}_o+\delta\boldsymbol{r}_o) &= \mathbf{F}_{io}(\boldsymbol{r}_i+\delta\boldsymbol{r}_i,\boldsymbol{r}_o+\delta\boldsymbol{r}_o)+\mathbf{F}_{gi}(\boldsymbol{r}_i+\delta\boldsymbol{r}_i)\\
&= \Big(\mathbf{F}_{io}(\boldsymbol{r}_i,\boldsymbol{r}_o)+\frac{\partial\mathbf{F}_{io}(\boldsymbol{r}_i,\boldsymbol{r}_o)}{\partial\boldsymbol{r}_i}\delta\boldsymbol{r}_i+\frac{\partial\mathbf{F}_{io}(\boldsymbol{r}_i,\boldsymbol{r}_o)}{\partial\boldsymbol{r}_o}\delta\boldsymbol{r}_o\Big)+\Big(\mathbf{F}_{gi}(\boldsymbol{r}_i)+\frac{\partial\mathbf{F}_{gi}(\boldsymbol{r}_i)}{\partial\boldsymbol{r}_i}\delta\boldsymbol{r}_i\Big)\\
&\overset{(30)}{=} \Big(\frac{\partial\mathbf{F}_{io}(\boldsymbol{r}_i,\boldsymbol{r}_o)}{\partial\boldsymbol{r}_i}\delta\boldsymbol{r}_i+\frac{\partial\mathbf{F}_{io}(\boldsymbol{r}_i,\boldsymbol{r}_o)}{\partial\boldsymbol{r}_o}\delta\boldsymbol{r}_o\Big)+\Big(\frac{\partial\mathbf{F}_{gi}(\boldsymbol{r}_i)}{\partial\boldsymbol{r}_i}\delta\boldsymbol{r}_i\Big)\\
&\overset{(31)}{=} \Big(\frac{\partial\mathbf{F}_{io}(\boldsymbol{r}_i,\boldsymbol{r}_o)}{\partial\boldsymbol{r}_i}\delta_0(\boldsymbol{r}_i-\boldsymbol{r}_{gi})^{\perp}+\frac{\partial\mathbf{F}_{io}(\boldsymbol{r}_i,\boldsymbol{r}_o)}{\partial\boldsymbol{r}_o}(-\delta_1(\boldsymbol{r}_i-\boldsymbol{r}_{gi})^{\perp}+\delta_2(\boldsymbol{r}_i-\boldsymbol{r}_{gi})^{\parallel})\Big)\\
&\quad+\Big(\frac{\partial\mathbf{F}_{gi}(\boldsymbol{r}_i)}{\partial\boldsymbol{r}_i}\delta_0(\boldsymbol{r}_i-\boldsymbol{r}_{gi})^{\perp}\Big)\\
&\overset{(3),(4)}{=} \Big(\frac{\mathbf{I}d_{io}^2-\boldsymbol{r}_{oi}\boldsymbol{r}_{oi}^T}{d_{io}^3}\delta_0(\boldsymbol{r}_i-\boldsymbol{r}_{gi})^{\perp}-\frac{\mathbf{I}d_{io}^2-\boldsymbol{r}_{oi}\boldsymbol{r}_{oi}^T}{d_{io}^3}(-\delta_1(\boldsymbol{r}_i-\boldsymbol{r}_{gi})^{\perp}+\delta_2(\boldsymbol{r}_i-\boldsymbol{r}_{gi})^{\parallel})\Big)\\
&\quad+\Big(\frac{-\mathbf{I}d_{gi}^2+(\boldsymbol{r}_i-\boldsymbol{r}_{gi})(\boldsymbol{r}_i-\boldsymbol{r}_{gi})^T}{d_{gi}^3}\delta_0(\boldsymbol{r}_i-\boldsymbol{r}_{gi})^{\perp}\Big),
\end{aligned}$$

where $d_{gi}=\|\boldsymbol{r}_i-\boldsymbol{r}_{gi}\|$, $\boldsymbol{r}_{oi}=\boldsymbol{r}_i-\boldsymbol{r}_o$ and $\mathbf{I}\in\mathbb{R}^{2\times2}$ is the identity matrix. Note that $\boldsymbol{r}_{oi}$ is also along $(\boldsymbol{r}_i-\boldsymbol{r}_{gi})^{\parallel}$ and hence, it is perpendicular to $(\boldsymbol{r}_i-\boldsymbol{r}_{gi})^{\perp}$. Using this, we obtain:

$$\begin{aligned}
\mathbf{F}_i(\boldsymbol{r}_i+\delta\boldsymbol{r}_i,\boldsymbol{r}_o+\delta\boldsymbol{r}_o) &= \Big(\frac{\delta_0(\boldsymbol{r}_i-\boldsymbol{r}_{gi})^{\perp}}{d_{io}}+\frac{\delta_1(\boldsymbol{r}_i-\boldsymbol{r}_{gi})^{\perp}}{d_{io}}-\frac{\mathbf{I}d_{io}^2-\boldsymbol{r}_{oi}\boldsymbol{r}_{oi}^T}{d_{io}^3}(\delta_2(\boldsymbol{r}_i-\boldsymbol{r}_{gi})^{\parallel})\Big)+\frac{-\delta_0(\boldsymbol{r}_i-\boldsymbol{r}_{gi})^{\perp}}{d_{gi}}\\
&= \Big(\frac{\delta_0(\boldsymbol{r}_i-\boldsymbol{r}_{gi})^{\perp}}{d_{io}}+\frac{\delta_1(\boldsymbol{r}_i-\boldsymbol{r}_{gi})^{\perp}}{d_{io}}-\frac{\delta_0(\boldsymbol{r}_i-\boldsymbol{r}_{gi})^{\perp}}{d_{gi}}-\frac{\mathbf{I}d_{io}^2-\boldsymbol{r}_{oi}\boldsymbol{r}_{oi}^T}{d_{io}^3}(\delta_2(\boldsymbol{r}_i-\boldsymbol{r}_{gi})^{\parallel})\Big).
\end{aligned}$$

Also note that $(\mathbf{I}d_{io}^2-\boldsymbol{r}_{oi}\boldsymbol{r}_{oi}^T)\delta_2(\boldsymbol{r}_i-\boldsymbol{r}_{gi})^{\parallel}=\delta_2 d_{io}^2(\boldsymbol{r}_i-\boldsymbol{r}_{gi})^{\parallel}-\delta_2\boldsymbol{r}_{oi}\boldsymbol{r}_{oi}^T(\boldsymbol{r}_i-\boldsymbol{r}_{gi})^{\parallel}=\mathbf{0}$ for all $\boldsymbol{r}_{oi}$. Hence, for $\mathbf{F}_i(\boldsymbol{r}_i+\delta\boldsymbol{r}_i,\boldsymbol{r}_o+\delta\boldsymbol{r}_o)=\mathbf{0}$ to hold, we need:

$$\frac{\delta_0+\delta_1}{d_{io}}=\frac{\delta_0}{d_{gi}}.$$

Hence, it is needed that:

$$d_{gi}=\frac{\delta_0}{\delta_0+\delta_1}d_{io}<d_{io}.$$

Since the agent o is in the sensing radius of the agent i, we obtain that $d_{gi}<d_{io}<R_c$. Using the same set of arguments as above for some other agent j from the rest of the $K-1$ agents, we can obtain $d_{gj}<d_{jo'}<R_c$, where o' is the auxiliary agent corresponding to agent j. Since the repulsive forces for the agents i and j cancel out the attractive fields towards their respective goal location, we obtain that their goal locations $\boldsymbol{r}_{gi}$ and $\boldsymbol{r}_{gj}$ are located towards their front, using which we obtain $\|\boldsymbol{r}_{gi}-\boldsymbol{r}_{gj}\|\leq R_c$, which violates Assumption 3. Hence, if the goal locations are chosen as per Assumption 3, the condition $d_{gi}=\frac{\delta_0}{\delta_0+\delta_1}d_{io}$ would never hold, and hence, we have that $\mathbf{F}_i(\boldsymbol{r}_i+\delta\boldsymbol{r}_i,\boldsymbol{r}_o+\delta\boldsymbol{r}_o)\neq\mathbf{0}$.

Furthermore, we note that from Assumption 3, there is at least one agent i out of the K agents such that $d_{gi} > d_{ij}$, which implies that $\mathbf{F}_i(\boldsymbol{r}_i + \delta\boldsymbol{r}_i, \boldsymbol{r}_o + \delta\boldsymbol{r}_o)$ is along $(\boldsymbol{r}_i - \boldsymbol{r}_{gi})^{\perp}$, making agent i move away from the position $\boldsymbol{r}_i$ for which $\mathbf{F}_i(\boldsymbol{r}_i) = 0$, which completes the proof. □

B. Proof of Theorem 4

Proof. Define $\boldsymbol{z}(t) = \begin{bmatrix} \boldsymbol{r}_{ie}(t)^T & \boldsymbol{u}_{ie}(t)^T \end{bmatrix}^T$. First, note that the *nominal* error dynamics, i.e. when the disturbance $\boldsymbol{w}(\boldsymbol{r}_i, t) = 0$, the origin is finite-time stable for the system (15). Using [47, Theorems 4.1, 6.2], we have that there exists a function $T(\boldsymbol{r}_{ie}, \boldsymbol{u}_{ie})$ that is continuous at origin. Now, using this function as the settling time, from [46, Theorem 4.3], we have that there exists a continuous Lyapunov function $V(\boldsymbol{r}_{ie}, \boldsymbol{u}_{ie})$ satisfying the condition $\dot{V}(\boldsymbol{r}_{ie}, \boldsymbol{u}_{ie}) + c(V(\boldsymbol{r}_{ie}, \boldsymbol{u}_{ie}))^{\beta} \leq 0$, for some $c > 0$ and $0 < \beta < 1$ (namely, $V(\boldsymbol{r}_{ie}, \boldsymbol{u}_{ie}) = (T(\boldsymbol{r}_{ie}, \boldsymbol{u}_{ie}))^{\frac{1}{1-\beta}}$). Let β satisfy $\beta \in (0, \frac{1}{2})$. Since $\|\boldsymbol{w}(\boldsymbol{r}_i, t) - \boldsymbol{w}_{av}\| \leq \delta_w$, using [46, Theorem 5.2], we obtain that with $\boldsymbol{z}(0) \in \mathcal{U}$, where $\mathcal{U}$ is an open neighbourhood of origin, $\boldsymbol{z}(t) \in \mathcal{U}$ for all time $t \geq 0$. Define $\mathcal{U} = \{z \mid \|z\| \leq \|\boldsymbol{z}(0)\|\}$ so that $\boldsymbol{z}(0) \in \mathcal{U}$. Since we can choose $\hat{\boldsymbol{r}}_i(0) = \boldsymbol{r}_i(0)$, we have that $\|\boldsymbol{z}(t)\| \leq \|\boldsymbol{z}(0)\| = \|\boldsymbol{u}_{ie}(0)\|$. From this, we have that $\|\boldsymbol{z}(t)\| \leq \|\boldsymbol{u}_{ie}(0)\|$ for all time $t \geq 0$. Furthermore, again as per [46, Theorem 5.2], there exists a finite time T_i^{obs} such that for all $t \geq T_i^{obs}$

$$\|\boldsymbol{z}(t)\| \leq l_i \delta_w^{c_i}, \tag{32}$$

where $l_i = ((2(1-\beta))^{\frac{1-\beta}{\beta}} \|\boldsymbol{u}_{ie}(0)\| > 0$, $c_i = \frac{1-\beta}{\beta} > 1$. Hence, with choice of $\delta_{ie}(t)$ as per (16), we obtain that $\|\boldsymbol{z}(t)\| \leq \delta_{ie}(t)$ for all $t \geq 0$. □

C. Proof of Theorem 5

Proof. Before we prove the safety, we note that the following inequality holds for all $t \geq 0$ and for all $i \neq j$:

$$\hat{d}_{ij} = \|\hat{\boldsymbol{r}}_i - \boldsymbol{r}_{js}^i\| \leq \|\hat{\boldsymbol{r}}_i - \boldsymbol{r}_i\| + \|\boldsymbol{r}_{js}^i - \boldsymbol{r}_j\| + \|\boldsymbol{r}_i - \boldsymbol{r}_j\| \leq \delta_e + \epsilon_s + \|\boldsymbol{r}_i - \boldsymbol{r}_j\|,$$

which means that if $\hat{d}_{ij} = \|\hat{\boldsymbol{r}}_i - \boldsymbol{r}_{js}^i\| \geq d_m + \epsilon_s + \delta_e$, then $d_{ij} = \|\boldsymbol{r}_i - \boldsymbol{r}_j\| \geq d_m$. Hence, we need to prove that $\hat{d}_{ij} \geq d_m + \epsilon_s + \delta_e$ holds for all time $t \geq 0$. From Assumption 3, we have that the inter-agent distance $d_{ij}(0) \geq d_m$ which means that all the agents start from a safe distance. Let j be some agent in the sensing region of the agent i at some time instant $t \geq 0$, i.e., $\hat{d}_{ij}(t) \leq R_c$. Denote the steady-state values of the $\hat{\boldsymbol{r}}_i$ and $\hat{\boldsymbol{u}}_i$ as $\hat{\boldsymbol{r}}_i^{ss}$ and $\hat{\boldsymbol{u}}_i^{ss}$, respectively. Note that the steady-state velocity satisfy $\hat{\boldsymbol{u}}_i^{ss} = \boldsymbol{u}_{id}$. Consider the time derivative of the estimated distance, which in the steady state (i.e. when $\hat{\boldsymbol{u}}_i = \hat{\boldsymbol{u}}_{id}$ and $\hat{\boldsymbol{r}}_i = \hat{\boldsymbol{r}}_i^{ss}$) reads:

$$\dot{\hat{d}}_{ij} = \frac{\hat{u}_{id}\,(\hat{\boldsymbol{r}}_i^{ss} - \boldsymbol{r}_{js}^i)^T \hat{\boldsymbol{u}}_{idn} - (\hat{\boldsymbol{r}}_i^{ss} - \boldsymbol{r}_{js}^i)^T \boldsymbol{u}_{js}^i}{\hat{d}_{ij}^{ss}}. \tag{33}$$

The worst-case neighbor is the agent $j \in \{\mathcal{N}_i \mid \hat{J}_i < 0\}$ towards whom the rate of change of the estimated distance $\hat{d}_{ij}$ given by (33), due to the motion of agent i, is maximum. More specifically, the term $\hat{J}_i < 0$ describes the set of agents $j \in \mathcal{N}_i$ towards whom agent i is moving in its current direction (see [9] for more details). Consider the worst case, i.e., $\hat{d}_{ij}^{ss} = \|\hat{\boldsymbol{r}}_i^{ss} - \boldsymbol{r}_{js}^i\| = d_s$. The commanded speed $\hat{u}_{id}$ in this case is equal to $\hat{u}_{is|j}$ which is given as per (21). Plugging this into (33), we obtain:

$$\dot{\hat{d}}_{ij} = \frac{(1-\varepsilon_i)u_e d_s + (\varepsilon_i - 1)(\hat{\boldsymbol{r}}_i - \boldsymbol{r}_{js}^i)^T \boldsymbol{u}_{js}^i}{d_s} \tag{34}$$

Note that

$$(\hat{\boldsymbol{r}}_i - \boldsymbol{r}_{js}^i)^T \boldsymbol{u}_{js}^i = (\hat{\boldsymbol{r}}_i - \hat{\boldsymbol{r}}_j)^T \boldsymbol{u}_{js}^i + (\hat{\boldsymbol{r}}_j - \hat{\boldsymbol{r}}_{js})^T \boldsymbol{u}_{js}^i = (\hat{\boldsymbol{r}}_i - \hat{\boldsymbol{r}}_j)^T \hat{\boldsymbol{u}}_j + (\hat{\boldsymbol{r}}_i - \hat{\boldsymbol{r}}_j)^T (\boldsymbol{u}_{js}^i - \hat{\boldsymbol{u}}_j) + (\hat{\boldsymbol{r}}_j - \hat{\boldsymbol{r}}_{js})^T \boldsymbol{u}_{js}^i.$$

Using the fact that either the agent j is moving away from the agent i at the first place or is following the vector field that points away from agent i, we have $(\hat{\boldsymbol{r}}_i - \hat{\boldsymbol{r}}_j)^T \hat{\boldsymbol{u}}_j \leq 0$ (where $\hat{\boldsymbol{u}}_j$ is the estimated velocity of agent j, available only to agent j). Furthermore, using the bounds on the estimation and sensing errors, we obtain

$$(\hat{\boldsymbol{r}}_i - \hat{\boldsymbol{r}}_j)^T \hat{\boldsymbol{u}}_j + (\hat{\boldsymbol{r}}_i - \hat{\boldsymbol{r}}_j)^T (\boldsymbol{u}_{js}^i - \hat{\boldsymbol{u}}_j) + (\hat{\boldsymbol{r}}_j - \hat{\boldsymbol{r}}_{js})^T \boldsymbol{u}_{js}^i \leq (d_s + \epsilon_s)(\delta_e + \epsilon_s) + \epsilon_s \|\boldsymbol{u}_{js}^i\|.$$

Choose u_e as

$$u_e = \frac{(d_s + \epsilon_s)(\delta_e + \epsilon_s) + \epsilon_s \|\boldsymbol{u}_{js}^i\|}{d_s} \tag{35}$$

Now, from (34) and choice of u_e as per (35), we have

$$(1-\varepsilon_i)u_e d_s + (\varepsilon_i - 1)(\hat{\boldsymbol{r}}_i - \boldsymbol{r}_{js}^i)^T \boldsymbol{u}_{js}^i \geq (1-\varepsilon_i)u_e d_s - (1-\varepsilon_i)\big((d_s + \epsilon_s)(\delta_e + \epsilon_s) + \epsilon_s \|\boldsymbol{u}_{js}^i\|\big) \geq 0,$$

which implies that the steady-state estimated inter-agent distance $\hat{d}_{ij}^{ss}$ can not become less than d_s. Now, to account for the transient period, consider the time derivative of the velocity error $\hat{\boldsymbol{u}}_{ide}$, which reads

$$\dot{\hat{\boldsymbol{u}}}_{ide} = \dot{\hat{\boldsymbol{u}}}_i - \dot{\hat{\boldsymbol{u}}}_{id} = \boldsymbol{a}_i + k_{i4} \boldsymbol{r}_{ie} \|\boldsymbol{r}_{ie}\|^{\alpha_2 - 1} - \dot{\hat{\boldsymbol{u}}}_{id} \tag{36}$$

Substituting (22) into (36) yields

$$\dot{\hat{\boldsymbol{u}}}_{ide} = -\lambda_i (\hat{\boldsymbol{u}}_i - \hat{\boldsymbol{u}}_{id}) \|\hat{\boldsymbol{u}}_i - \hat{\boldsymbol{u}}_{id}\|^{\beta_2 - 1} = -\lambda_i \boldsymbol{u}_{ide} \|\boldsymbol{u}_{ide}\|^{\beta_2 - 1}, \tag{37}$$

where $\lambda_i > 0$. From Theorem 3, we obtain that the origin is a finite-time stable equilibrium of the system (37). Integrating equation (37) furthermore yields

$$\boldsymbol{u}_{ide}(t) = \boldsymbol{u}_{ide}(0)\Big(1 - \frac{\lambda_i t(1-\beta_2)}{\|\boldsymbol{u}_{ide}(0)\|^{1-\beta_2}}\Big)^{\frac{1}{1-\beta_2}} = c_1(1-c_2 t)^{\xi} \tag{38}$$

where, $\boldsymbol{u}_{ide}(0)$ is the initial velocity error, $c_1 = \boldsymbol{u}_{ide}(0)$, $c_2 = \frac{\lambda_i(1-\beta_2)}{\|\boldsymbol{u}_{ide}(0)\|^{1-\beta_2}}$, and $\xi = \frac{1}{1-\beta_2}$. Note that $\boldsymbol{u}_{ide}(t) = 0$ for all $t \geq t^* = \frac{1}{c_2}$. Hence, after this instant, the error in position would not change. By integrating (38), we obtain the transient position error $\boldsymbol{r}_{ide}(t)$ as

$$\boldsymbol{r}_{ide}(t) = \boldsymbol{r}_{ide}(0) + \frac{c_1}{c_2(1+\xi)}(1-(1-c_2 t)^{1+\xi}) \tag{39}$$

With $\boldsymbol{r}_{ide}(0) = 0$, the maximum position error $\boldsymbol{r}_{ieMax}$, attained at $t^* = \frac{1}{c_2}$, has the form

$$\boldsymbol{r}_{ieMax} = \boldsymbol{r}_{ide}\Big(\frac{1}{c_2}\Big) = \frac{c_1}{c_2(1+\xi)} = \frac{\boldsymbol{u}_{ide}(0)\|\boldsymbol{u}_{ide}(0)\|^{1-\beta_2}}{\lambda_i(2-\beta_2)},$$

where $\boldsymbol{u}_{ide}(0) = \hat{\boldsymbol{u}}_i(0) - u_{id}(0)\boldsymbol{u}_{idn}(0) + \boldsymbol{w}_{av} + k_{i3}\boldsymbol{r}_{ie}(0)\|\boldsymbol{r}_{ie}(0)\|^{\alpha_1 - 1}$. Define r_e as

$$r_e = \max_i \|\boldsymbol{r}_{ieMax}\|. \tag{40}$$

Note that from the steady-state analysis, we have that $\|\hat{\boldsymbol{r}}_i^{ss} - \hat{\boldsymbol{r}}_{js}\| \geq d_s$. Using this, we obtain:

$$\hat{d}_{ij} = \|\hat{\boldsymbol{r}}_i - \hat{\boldsymbol{r}}_{js}\| \geq \|\hat{\boldsymbol{r}}_i^{ss} - \hat{\boldsymbol{r}}_{js}\| - \|\hat{\boldsymbol{r}}_i - \hat{\boldsymbol{r}}_i^{ss}\| \geq d_s - r_e$$

Thus, with $d_s = d_m + \delta_e + \epsilon_s + r_e$, we have that $\hat{d}_{ij} \geq d_m + \delta_e + \epsilon_s$ and hence, $d_{ij} \geq d_m$, i.e., the resulting agent trajectories are collision free. □

D. Proof of Lemma 4

Proof. Let $V(\boldsymbol{x}) = \frac{1}{2}\|\boldsymbol{x}(t)\|^2$ be the candidate Lyapunov function. Taking the time derivative of $V(\boldsymbol{x})$ along the system trajectories, we obtain

$$\dot{V}(\boldsymbol{x}) = \boldsymbol{x}(t)^T(-k\boldsymbol{x}(t)\frac{\tanh\|\boldsymbol{x}(t)\|}{\|\boldsymbol{x}(t)\|}) = -k\|\boldsymbol{x}(t)\|\tanh(\|\boldsymbol{x}(t)\|).$$

This shows that $\dot{V}(\boldsymbol{x}(t)) < 0$ for all $\boldsymbol{x}(t) \neq \boldsymbol{0}$. Hence, we have that $V(\boldsymbol{x}(t)) \leq V(\boldsymbol{x}(0))$ or $\|\boldsymbol{x}(t)\| \leq \|\boldsymbol{x}(0)\|$ for all $t \geq 0$. Define $x_0 \triangleq \|\boldsymbol{x}(0)\|$ so that we have $\|\boldsymbol{x}(t)\| \leq x_0$ and since $\boldsymbol{x}(0) \neq \boldsymbol{0}$, $x_0 > 0$. It is easy to check that the system trajectories satisfy $\tanh(\|\boldsymbol{x}(t)\|) \geq \frac{\tanh(x_0)}{x_0}\|\boldsymbol{x}(t)\|$ for all $t \geq 0$, i.e., the graph of $\tanh(\|\boldsymbol{x}(t)\|)$ lies above the straight

line $y = c\|\boldsymbol{x}(t)\|$ with slope $c = \frac{\tanh(x_0)}{x_0}$ for all $\|\boldsymbol{x}(t)\| \leq x_0$. Hence, we have that $\dot{V}(\boldsymbol{x}) = -k\|\boldsymbol{x}(t)\|\tanh(\|\boldsymbol{x}(t)\|) \leq -\frac{k\tanh(x_0)}{x_0}\|\boldsymbol{x}(t)\|^2 = -cV(\boldsymbol{x})$ where $c = \frac{2k\tanh(x_0)}{x_0}$. From the Comparison Lemma [61, Section 5.2], we obtain that $V(\boldsymbol{x}(t)) \leq e^{-ct}V(\boldsymbol{x}(0))$.

For a given $\epsilon > 0$, define $T_\epsilon = -\frac{1}{c}\log(\frac{\epsilon^2}{2V(\boldsymbol{x}(0))})$, so that we have $V(\boldsymbol{x}(T_\epsilon)) \leq e^{-cT_\epsilon}V(\boldsymbol{x}(0)) = \frac{1}{2}\epsilon^2$. Now, since $V(\boldsymbol{x}(t)) \leq V(\boldsymbol{x}(T_\epsilon))$ for all $t \geq T_\epsilon$, we obtain that $V(\boldsymbol{x}(t)) \leq \frac{1}{2}\epsilon^2$ or $\|\boldsymbol{x}(t)\| \leq \epsilon$ for all $t \geq T_\epsilon$. Also, since $\|\boldsymbol{x}_0\| \neq 0$, we have that $T_\epsilon < \infty$. □

E. Proof of Theorem 6

Proof. From Lemma 1, there is no deadlock so that the agents are always attracted to their desired goal locations. The agents follow the vector field (6) under the desired direction of motion given by (7), which takes each agent i away from the other agents and towards its goal location, i.e., each class-A agent resolves the conflict with all other agents. Also, from Assumption 3, once all agents reach their respective goal locations, they are out of each others' sensing region. Hence, once all the agents reached to their respective goal locations, they stay there.

Now, we are ready to show that once agent i resolves all its conflicts with the other agents, it would reach its goal location in finite time. Consider the error dynamics for $\hat{\boldsymbol{u}}_{ide}$ which, as per (37), reads $\dot{\hat{\boldsymbol{u}}}_{ide} = -\lambda_i(\boldsymbol{u}_{ide})\|\boldsymbol{u}_{ide}\|^{\beta_2-1}$. From Theorem 3, we have that the origin of the system (37) is FTS, which implies that there exists a time t_i such that for all $t \geq t_i$, $\hat{\boldsymbol{u}}_i(t) = \boldsymbol{u}_{id}(t)$. Note that from (17) and (14), we obtain $\dot{\hat{\boldsymbol{r}}}_i(t) = \hat{u}_{id}\hat{\boldsymbol{u}}_{idn}$ for all $t \geq t_i$. Now, in the absence of any neighbours, from (17), we have that $\hat{u}_{id} = \hat{u}_{ic}$ and the direction of vector field $\hat{\boldsymbol{u}}_{idn}$ is along $\mathbf{F}_i(\hat{\boldsymbol{r}}_i) = \mathbf{F}_{gi}(\hat{\boldsymbol{r}}_i)$, i.e., along $-(\hat{\boldsymbol{r}}_i - \boldsymbol{r}_{gi})$. Hence, the dynamics of the desired trajectory $\hat{\boldsymbol{r}}_{id}$ reads

$$\dot{\hat{\boldsymbol{r}}}_i = -\hat{u}_{ic}\frac{(\hat{\boldsymbol{r}}_i - \boldsymbol{r}_{gi})}{\|\hat{\boldsymbol{r}}_i - \boldsymbol{r}_{gi}\|}. \tag{41}$$

Now, if at the instant when the error $\hat{\boldsymbol{u}}_{ide}(t)$ becomes $\mathbf{0}$, the value of the norm $\|\hat{\boldsymbol{r}}_i - \boldsymbol{r}_{gi}\| \leq R_1$, then $\hat{u}_{ic}$ in (41) directly takes the form $\hat{u}_{ic} = k_{i2}\|\hat{\boldsymbol{r}}_i - \boldsymbol{r}_{gi}\|^{\alpha_r}$. If this is not the case, then by Lemma 4, there exits a finite time $\tilde{t}_i$, after which $\|\hat{\boldsymbol{r}}_i - \boldsymbol{r}_{gi}\|$ is less than R_1. Now, after this point, the value $\hat{u}_{ic}$ as per (10a) reads $\hat{u}_{ic} = k_{i2}\|\hat{\boldsymbol{r}}_i - \boldsymbol{r}_{gi}\|^{\alpha_r}$. Hence, we obtain

$$\dot{\hat{\boldsymbol{r}}}_i = -k_{i2}\|\hat{\boldsymbol{r}}_i - \boldsymbol{r}_{gi}\|^{\alpha_r}\frac{(\hat{\boldsymbol{r}}_i - \boldsymbol{r}_{gi})}{\|\hat{\boldsymbol{r}}_i - \boldsymbol{r}_{gi}\|} = -k_{i2}(\hat{\boldsymbol{r}}_i - \boldsymbol{r}_{gi})\|\hat{\boldsymbol{r}}_i - \boldsymbol{r}_{gi}\|^{\alpha_r-1}. \tag{42}$$

From Theorem 3, $\boldsymbol{r}_{gi}$ is a finite-time stable equilibrium for (42). Hence, there exists some finite-time T_i^* such that, for all $t \geq T_i^*$, $\hat{\boldsymbol{r}}_i = \boldsymbol{r}_{gi}$. Now, from Theorem 4, $\|\boldsymbol{r}_i(t) - \hat{\boldsymbol{r}}_i(t)\| \leq \delta_{ie}(t)$ for all $t \geq T_i^{obs}$. Define $T_i = \max\{T_i^*, T_i^{obs}\} < \infty$, so that for all $t \geq T_i$, $\|\boldsymbol{r}_i(t) - \hat{\boldsymbol{r}}_i(t)\| = \|\boldsymbol{r}_i(t) - \boldsymbol{r}_{gi}\| \leq \delta_{ie}(t)$, which completes the proof. □

Acknowledgments

The authors would like to acknowledge the support of the NASA Grant NNX16AH81A and the Air Force Office of Scientific Research under award number FA9550-17-1-0284. The authors would also like to thank the associate editor and the anonymous reviewers for their valuable comments and suggestions to improve the quality of the paper.

References

[1] Klausen, K., Fossen, T. I., Johansen, T. A., and Aguiar, A. P., "Cooperative Path-following for Multirotor UAVs with a Suspended Payload," *IEEE Conference on Control Applications*, 2015, pp. 1354–1360. doi:10.1109/CCA.2015.7320800.

[2] Quintero, S. A., Collins, G. E., and Hespanha, J. P., "Flocking with Fixed-wing UAVs for Distributed Sensing: A Stochastic Optimal Control Approach," *IEEE American Control Conference*, 2013, pp. 2025–2031. doi:10.1109/ACC.2013.6580133.

[3] Ren, W., and Cao, Y., "Overview of Recent Research in Distributed Multi-agent Coordination," *Distributed Coordination of Multi-agent Networks*, Communications and Control Engineering, Springer-Verlag, 2011, Chap. 2, pp. 23–41. doi: 10.1109/TII.2012.2219061.

[4] Knorn, S., Chen, Z., and Middleton, R. H., "Overview: Collective Control of Multiagent Systems," *IEEE Transactions on Control of Network Systems*, Vol. 3, No. 4, 2016, pp. 334–347. doi:10.1109/TCNS.2015.2468991.

[5] Peterson, C., and Paley, D. A., "Multivehicle Coordination in an Estimated Time-varying Flowfield," *Journal of guidance, control, and dynamics*, Vol. 34, No. 1, 2011, pp. 177–191. doi:10.2514/1.50036.

[6] Lee, J.-W., Walker, B., and Cohen, K., "Path Planning of Unmanned Aerial Vehicles in a Dynamic Environment," *Infotech@ Aerospace 2011*, AIAA, 2011, p. 1654. doi:10.2514/6.2011-1654.

[7] Alonso-Mora, J., Naegeli, T., Siegwart, R., and Beardsley, P., "Collision Avoidance for Aerial Vehicles in Multi-Agent Scenarios," *Autonomous Robots*, Vol. 39, No. 1, 2015, pp. 101–121. doi:10.1007/s10514-015-9429-0.

[8] Chen, Y., Cutler, M., and How, J. P., "Decoupled Multiagent Path Planning via Incremental Sequential Convex Programming," *IEEE International Conference on Robotics and Automation*, 2015, pp. 5954–5961. doi:10.1109/ICRA.2015.7140034.

[9] Panagou, D., Stipanović, D. M., and Voulgaris, P. G., "Distributed Coordination Control for Multi-Robot Networks using Lyapunov-like Barrier Functions," *IEEE Transactions on Automatic Control*, Vol. 61, No. 3, 2016, pp. 617–632. doi: 10.1109/TAC.2015.2444131.

[10] Glotfelter, P., Cortés, J., and Egerstedt, M., "Nonsmooth Barrier Functions With Applications to Multi-Robot Systems," *IEEE Control Systems Letters*, Vol. 1, No. 2, 2017, pp. 310–315. doi:10.1109/LCSYS.2017.2710943.

[11] Choi, J.-w., Curry, R., and Elkaim, G., "Real-time Obstacle-Avoiding Path Planning for Mobile Robots," *AIAA Guidance, Navigation, and Control Conference*, 2010, p. 8411. doi:10.2514/6.2010-8411.

[12] Wilburm, J., Perhinschi, M., Wilburn, B., and Karas, O., "Development of a Modified Voronoi Algorithm for UAV Path Planning and Obstacle Avoidance," *AIAA Guidance, Navigation, and Control Conference*, 2012, pp. 4904–4915. doi:10.2514/6.2012-4904.

[13] Chen, T., Zhang, G., Hu, X., and Xiao, J., "Unmanned Aerial Vehicle Route Planning Method Based on A-Star Algorithm," *2018 13th IEEE Conference on Industrial Electronics and Applications*, 2018, pp. 1510–1514. doi:10.1109/ICIEA.2018.8397948.

[14] Chen, G., Shen, D., Cruz, J., Kwan, C., Riddle, S., Cox, S., and Matthews, C., "A Novel Cooperative Path Planning for Multiple Aerial Platforms," *Infotech@ Aerospace*, AIAA, 2005, p. 6948. doi:10.2514/6.2005-6948.

[15] Aoude, G. S., Luders, B. D., Joseph, J. M., Roy, N., and How, J. P., "Probabilistically Safe Motion Planning to Avoid Dynamic Obstacles with Uncertain Motion Patterns," *Autonomous Robots*, Vol. 35, No. 1, 2013, pp. 51–76. doi:10.1007/s10514-013-9334-3.

[16] Frazzoli, E., Dahleh, M. A., and Feron, E., "Real-time Motion Planning for Agile Autonomous Vehicles," *Journal of Guidance, Control, and Dynamics*, Vol. 25, No. 1, 2002, pp. 116–129. doi:10.2514/2.4856.

[17] Elbanhawi, M., and Simic, M., "Sampling-Based Robot Motion Planning: A Review," *IEEE Access*, Vol. 2, 2014, pp. 56–77. doi:10.1109/ACCESS.2014.2302442.

[18] LaValle, S. M., *Planning Algorithms*, Cambridge University Press, 2006. doi:10.1017/CBO9780511546877.

[19] Choset, H., Lynch, K., Hutchinson, S., Kantor, G., Burgard, W., Kavraki, L., and Thrun, S., *Principles of Robot Motion. Theory, Algorithms and Implementation*, MIT Press, 2005. doi:10.1017/S0263574706212803.

[20] Leitmann, G., and Skowronski, J., "Avoidance Control," *Journal of Optimization Theory and Applications*, Vol. 23, 1977, pp. 581–591. doi:10.1007/BF00933298.

[21] Hernandez-Martinez, E. G., and Aranda-Bricaire, E., "Convergence and Collision Avoidance in Formation Control: A Survey of the Artificial Potential Functions Approach," *Multi-Agent Systems - Modeling, Control, Programming, Simulations and Applications*, edited by F. Alkhateeb, E. A. Maghayreh, and I. A. Doush, InTech, 2011, Chap. 6, pp. 103–126. doi:10.5772/14142.

[22] Dimarogonas, D. V., and Kyriakopoulos, K. J., "Connectedness Preserving Distributed Swarm Aggregation for Multiple Kinematic Robots," *IEEE Transactions on Robotics*, Vol. 24, No. 5, 2008, pp. 1213–1223. doi:10.1109/TRO.2008.2002313.

[23] Cheng, T.-H., Kan, Z., Rosenfeld, J. A., and Dixon, W. E., "Decentralized Formation Control with Connectivity Maintenance and Collision Avoidance Under Limited and Intermittent Sensing," *IEEE American Control Conference*, 2014, pp. 3201–3206. doi:10.1109/ACC.2014.6859177.

[24] Szulczyński, P., Pazderski, D., and Kozłowski, K., "Real-Time Obstacle Avoidance using Harmonic Potential Functions," *Journal of Automation, Mobile Robotics and Intelligent Systems*, Vol. 5, No. 3, 2011, pp. 59–66.

[25] Liddy, T., Lu, T.-F., Lozo, P., and Harvey, D., "Obstacle Avoidance Using Complex Vector Fields," *Proc. of the 2008 Australasian Conference on Robotics and Automation*, Canberra, Australia, 2008.

[26] Hernández-Martínez, E. G., and Aranda-Bricaire, E., "Multi-agent Formation Control with Collision Avoidance Based on Discontinuous Vector Fields," *35th Annual Conference of IEEE Industrial Electronics*, 2009, pp. 2283–2288. doi: 10.1109/IECON.2009.5415217.

[27] Flores-Resendiz, J., Aranda-Bricaire, E., González-Sierra, J., and Santiaguillo-Salinas, J., "Finite-time Formation Control Without Collisions for Multiagent Systems with Communication Graphs Composed of Cyclic Paths," *Mathematical Problems in Engineering*, Vol. 2015, 2015. doi:10.1155/2015/948086.

[28] Rodríguez-Seda, E. J., Tang, C., Spong, M. W., and Stipanović, D. M., "Trajectory Tracking with Collision Avoidance for Nonholonomic Vehicles with Acceleration Constraints and Limited Sensing," *The International Journal of Robotics Research*, Vol. 33, No. 12, 2014, pp. 1569–1592. doi:10.1177/0278364914537130.

[29] Rodríguez-Seda, E. J., Stipanović, D. M., and Spong, M. W., "Guaranteed Collision Avoidance for Autonomous Systems with Acceleration Constraints and Sensing Uncertainties," *Journal of Optimization Theory and Applications*, Vol. 168, No. 3, 2016, pp. 1014–1038. doi:10.1007/s10957-015-0824-7.

[30] Panagou, D., "A Distributed Feedback Motion Planning Protocol for Multiple Unicycle Agents of Different Classes," *IEEE Transactions on Automatic Control*, Vol. 62, No. 3, 2017, pp. 1178–1193. doi:10.1109/TAC.2016.2576020.

[31] Ahn, H., Colombo, A., and Del Vecchio, D., "Supervisory Control for Intersection Collision Avoidance in the Presence of Uncontrolled Vehicles," *IEEE American Control Conference*, IEEE, 2014, pp. 867–873. doi:10.1109/ACC.2014.6859163.

[32] Ahn, H., Rizzi, A., Colombo, A., and Del Vecchio, D., "Robust Supervisors for Intersection Collision Avoidance in the Presence of Uncontrolled Vehicles," *arXiv preprint arXiv:1603.03916*, 2016.

[33] Trentelman, H. L., Takaba, K., and Monshizadeh, N., "Robust Synchronization of Uncertain Linear Multi-Agent Systems," *IEEE Transactions on Automatic Control*, Vol. 58, No. 6, 2013, pp. 1511–1523. doi:10.1109/TAC.2013.2239011.

[34] Liu, X., Ho, D. W., Cao, J., and Xu, W., "Discontinuous Observers Design for Finite-time Consensus of Multiagent Systems with External Disturbances," *IEEE Transactions on Neural Networks and Learning Systems*, Vol. 28, No. 11, 2017, pp. 2826–2830. doi:10.1109/TNNLS.2016.2599199.

[35] Fu, J., and Wang, J., "Fixed-time Coordinated Tracking for Second-order Multi-Agent Systems with Bounded Input Uncertainties," *Systems & Control Letters*, Vol. 93, 2016, pp. 1–12. doi:10.1016/j.sysconle.2016.03.006.

[36] Hong, H., Yu, W., Wen, G., and Yu, X., "Distributed Robust Fixed-time Consensus for Nonlinear and Disturbed Multiagent Systems," *IEEE Transactions on Systems, Man, and Cybernetics: Systems*, Vol. 47, No. 7, 2017, pp. 1464–1473. doi: 10.1109/TSMC.2016.2623634.

[37] Wang, X., and Li, S., "Distributed Finite-time Consensus Algorithms for Leader-follower Second-order Multi-Agent Systems with Mismatched Disturbances," *IEEE American Control Conference*, 2016, pp. 2814–2819. doi:10.1109/ACC.2016.7525345.

[38] Li, P., Qin, K., and Shi, M., "Distributed Robust H-infinity Rotating Consensus Control for Directed Networks of Second-order Agents with Mixed uUcertainties and Time-delay," *Neurocomputing*, Vol. 148, 2015, pp. 332–339. doi:10.1016/j.neucom.2014.06.063.

[39] Rezaei, V., and Stefanovic, M., "Distributed Leaderless and Leader-follower Consensus of Linear Multiagent Systems Under Persistent Disturbances," *24th Mediterranean Conference on Control and Automation*, IEEE, 2016, pp. 587–592. doi:10.1109/MED.2016.7536062.

[40] Wang, X., Saberi, A., Stoorvogel, A. A., and Grip, H. F., "Control of a Chain of Integrators Subject to Actuator Saturation and Disturbances," *International Journal of Robust and Nonlinear Control*, Vol. 22, No. 14, 2012, pp. 1562–1570. doi:10.1002/rnc.1767.

[41] Wang, X., Li, S., Yu, X., and Yang, J., "Distributed Active Anti-disturbance Consensus for Leader-follower Higher-order Multi-Agent Systems with Mismatched Disturbances," *IEEE Transactions on Automatic Control*, Vol. 62, No. 11, 2017, pp. 5795–5801. doi:10.1109/TAC.2016.2638966.

[42] Tian, B., Lu, H., Zuo, Z., and Zong, Q., "Multivariable Uniform Finite-Time Output Feedback Reentry Attitude Control for RLV with Mismatched Disturbance," *Journal of the Franklin Institute*, Vol. 355, No. 8, 2018. doi:10.1016/j.jfranklin.2018.01.042.

[43] Garg, K., Han, D., and Panagou, D., "Robust Semi-cooperative Multi-Agent Coordination in the Presence of Stochastic Disturbances," *IEEE 56th Annual Conference on Decision and Control*, 2017, pp. 3443–3448. doi:10.1109/CDC.2017.8264163.

[44] Garg, K., and Panagou, D., "A Robust Coordination Protocol for Safe Multi-Agent Motion Planning," *AIAA Guidance, Navigation, and Control Conference*, 2018, p. 0605. doi:10.2514/6.2018-0605.

[45] Ryan, E., "Finite-time Stabilization of Uncertain Nonlinear Planar Systems," *Dynamics and control*, Vol. 1, Springer, 1991, pp. 83–94. doi:10.1007/BF02169426.

[46] Bhat, S. P., and Bernstein, D. S., "Finite-time Stability of Continuous Autonomous Systems," *SIAM Journal on Control and Optimization*, Vol. 38, No. 3, 2000, pp. 751–766. doi:10.1137/S0363012997321358.

[47] Bhat, S. P., and Bernstein, D. S., "Geometric homogeneity with Applications to Finite-time Stability," *Mathematics of Control, Signals and Systems*, Vol. 17, No. 2, 2005, pp. 101–127. doi:10.1007/s00498-005-0151-x.

[48] Wang, X., and Hong, Y., "Finite-time Consensus for Multi-Agent Networks with Second-order Agent Dynamics," *IFAC Proceedings Volumes*, Vol. 41, No. 2, 2008, pp. 15185–15190. doi:10.3182/20080706-5-KR-1001.02568.

[49] Xiao, F., Wang, L., Chen, J., and Gao, Y., "Finite-time Formation Control for Multi-Agent Systems," *Automatica*, Vol. 45, No. 11, 2009, pp. 2605–2611. doi:10.1016/j.automatica.2009.07.012.

[50] Liu, Y., and Geng, Z., "Finite-time Formation Control for Linear Multi-Agent Systems: A Motion Planning Approach," *Systems & Control Letters*, Vol. 85, 2015, pp. 54–60. doi:10.1016/j.sysconle.2015.08.009.

[51] Li, S., and Wang, X., "Finite-time Consensus and Collision Avoidance Control Algorithms for Multiple AUVs," *Automatica*, Vol. 49, No. 11, 2013, pp. 3359–3367. doi:10.1016/j.automatica.2013.08.003.

[52] Li, S., Du, H., and Lin, X., "Finite-time Consensus Algorithm for Multi-Agent Systems with Double-integrator Dynamics," *Automatica*, Vol. 47, No. 8, 2011, pp. 1706–1712. doi:10.1016/j.automatica.2011.02.045.

[53] Hu, J., Li, S., Zhao, C., Pan, Q., Fan, B., Zhang, Z., and Li, H., "Finite-time Consensus for Multi UAV System with Collision Avoidance," *IEEE International Conference on Unmanned Systems*, IEEE, 2017, pp. 517–522. doi:10.1109/ICUS.2017.8278400.

[54] Ma, J., and Lai, E. M., "Finite-time Flocking Control of a Swarm of Cucker-Smale Agents with Collision Avoidance," *IEEE 24th International Conference on Mechatronics and Machine Vision in Practice*, 2017, pp. 1–6. doi:10.1109/M2VIP.2017.8211507.

[55] Wang, L., Sun, S., and Xia, C., "Finite-time Stability of Multi-Agent System in Disturbed Environment," *Nonlinear Dynamics*, Vol. 67, No. 3, 2012, pp. 2009–2016. doi:10.1007/s11071-011-0125-0.

[56] Zuo, Z., and Tie, L., "Distributed Robust Finite-time Nonlinear Consensus Protocols for Multi-Agent Systems," *International Journal of Systems Science*, Vol. 47, No. 6, 2016, pp. 1366–1375. doi:10.1080/00207721.2014.925608.

[57] Defoort, M., Polyakov, A., Demesure, G., Djemai, M., and Veluvolu, K., "Leader-follower Fixed-time Consensus for Multi-Agent Systems with Unknown Non-linear Inherent Dynamics," *IET Control Theory & Applications*, Vol. 9, No. 14, 2015, pp. 2165–2170. doi:10.1049/iet-cta.2014.1301.

[58] Ma, X., Jiao, Z., Wang, Z., and Panagou, D., "3-D Decentralized Prioritized Motion Planning and Coordination for High-Density Operations of Micro Aerial Vehicles," *IEEE Transactions on Control Systems Technology*, Vol. 26, No. 3, 2017, pp. 939–953. doi:10.1109/TCST.2017.2699165.

[59] Garg, K., and Panagou, D., "New Results on Finite-Time Stability: Geometric Conditions and Finite-Time Controllers," *IEEE Annual American Control Conference*, 2018, pp. 442–447. doi:10.23919/ACC.2018.8431699.

[60] Shen, Y., and Xia, X., "Semi-global Finite-time Observers for Nonlinear Systems," *Automatica*, Vol. 44, No. 12, 2008, pp. 3152–3156. doi:10.1016/j.automatica.2008.05.015.

[61] Kartsatos, A. G., *Advanced Ordinary Differential Equations*, Mariner, 1980.